SKELETAL MUSCLE PERICYTE RESPONSE TO ACUTE AND CHRONIC ELECTRICAL STIMULATION

BY

SVYATOSLAV DVORETSKIY

THESIS

Submitted in partial fulfillment of the requirements
for the degree of Master of Science in Kinesiology
in the Graduate College of the
University of Illinois at Urbana-Champaign, 2016

Urbana, Illinois

Master's Committee:

Associate Professor Marni Boppart
Assistant Professor Michael De Lisio

ABSTRACT

Pericytes are mural cells that are located on the outer surface of blood capillaries where they attach to endothelial cells and regulate vascular function, including dilation and angiogenesis. Recent studies suggest that pericytes in skeletal muscle may contribute to myofiber repair in response to injury. However, the pericyte response to exercise remains largely unexplored. **PURPOSE:** The purpose of this study was to evaluate pericyte quantity and gene expression in skeletal muscle following electrical stimulation, a method that can be used to simulate resistance exercise in mice. **METHODS:** Adult wild-type mice were subjected to an electrical stimulation protocol that results in 20 eccentric and 20 concentric contractions during a single session or (n=5; n=4 sham). A separate cohort of mixed-sex mice were subjected to electrical stimulation twice weekly for 4 weeks (n=4; n=4 sham) and 9 weeks (n=3; n=3 sham). At the end of each study, gastrocnemius-soleus complexes were dissected 24h following the final bout of stimulation. Pericyte quantity was assessed by multiplex flow cytometry in all samples. $NG2^{+}CD45^{-}CD31^{-}$ and $CD146^{+}CD45^{-}CD31^{-}$ pericytes were isolated following the acute study and gene expression was evaluated using high throughput qPCR. **RESULTS:** Acute electrical stimulation resulted in a non-significant trend for an increase in total pericyte content in skeletal muscle and a significant increase in the percentage of $NG2^{+}CD45^{-}CD31^{-}$ pericytes expressing the mesenchymal stem/stromal cell (MSC) marker CD140A. Isolation of pericytes based on CD146 revealed a population of cells highly engaged in the synthesis of factors necessary for myogenesis, satellite cell activation, and extracellular matrix remodeling post-acute stimulation. Finally, a pericyte to MSC transition was also observed with 4 weeks of stimulation, but no changes in overall pericyte quantity were noted at 4 or 9 weeks. **CONCLUSION:** This study provides evidence that resistance exercise promotes a pericyte to MSC transition, an event that may be necessary for pericytes to engage in skeletal muscle repair and adaptation.

ACKNOWLEDGEMENTS

I would like to thank my advisor Dr. Marni Boppart for giving me the opportunity to have a job that I truly enjoy. She is always available whenever I need help, whether it is related to teaching or research, she is always there to guide me in the right direction. I am very lucky to work for Dr. Boppart, as it is evident that she truly cares about her work and her students. I would also like to thank Dr. Michael De Lisio for being on my committee and offering additional advice with this project. I found that his Skeletal Muscle Physiology class has properly introduced me to the research process and helped me establish a firm foundation of knowledge to build on.

I would like to thank Yair Pincu for guiding me through the transition into graduate school. He taught me how to be an efficient graduate student and enjoy the process of research. Ziad has given me a tremendous amount of help relating to the writing process and has been a great leader in the laboratory, offering his help when I was swamped with this project. Michael has taught me and completed the work relating to flow cytometry and gene expression. I want to thank Brent Blackwell for his excellence as an undergraduate assistant. He was always available when I needed the most help and has always done an amazing job. I want to specifically thank Dr. Koyal Garg for being my greatest laboratory mentor thus far. Koyal has taught me the entire research process, from muscle dissection to data analysis.

I would like to thank my parents for even getting to this stage of my career. Their constant encouragement and financial support has been crucial to my overall progress. Lastly, I would like to thank my girlfriend Yuri Arroyo for her continued support and belief in my abilities.

TABLE OF CONTENTS

CHAPTER I

INTRODUCTION AND LITERATURE REVIEW

A) Pericytes

Pericytes are mural cells that are located on the outer surface of blood capillaries where they attach to endothelial cells. Pericytes are embedded into the capillary basal lamina and are fibroblast-like in their appearance as they wrap themselves around endothelial cells (Mills, 2013; Kostallari, 2015). A diagram of a pericyte and an endothelial cell is illustrated in Figure 1. Due to the plasticity of pericytes, these cells can express various markers in different tissues and at multiple stages of development (Mills, 2013). For these reasons, there is no single identifying marker for pericytes, although they typically express neuroglial 2 proteoglycan (NG2), CD146 and CD140B (Ozerdem, 2001; Armulik, 2011). Pericytes have high levels of α-smooth muscle actin and myosin, which suggests that they are able to regulate blood vessel contractility and blood flow (Mills, 2013).

Pericytes may also serve as multipotent stem cells that can differentiate into chondrocytes, adipocytes, osteoblasts, granulocytes and phagocytes (Hirschi, 1996; Mills, 2013). Although it is unclear if pericytes fulfill the definition of a multipotent stem cell with capacity for self-renewal and clonal expansion, studies suggest the ability for the pericyte to become myogenic and/or engage in skeletal muscle repair (Dellavalle, 2007). Two subpopulations of pericytes have been characterized in mouse skeletal muscle based on the expression of the proteoglycan NG2 and nestin, an intermediate filament protein expressed in dividing cells. Whereas Type 2 pericytes express nestin ($Nestin^{+}NG2^{+}$) and exhibit myogenic potential (Birbrair, 2013), Type 1 pericytes do not express nestin ($Nestin^{-}NG2^{+}$) and promote fibrogenesis and adipogenesis in response to injury. Type 2 pericyte involvement in myogenesis appears to

provide the canonical basis for pericyte-mediated repair. However, approximately 17% of Type 1 pericytes express CD140 (also PDGFRα) (Birbrair, 2013), suggesting potential for this fraction to exhibit a mesenchymal stem/stromal cell (MSC) phenotype with capacity to secrete regenerative paracrine factors necessary for healing. Investigators have suggested that pericytes can detach from capillaries and transition to a stromal cell with capacity to repair tissue post-injury (Caplan, 2008; Crisan, 2008), yet the essential experiments necessary to address this hypothesis have not been performed.

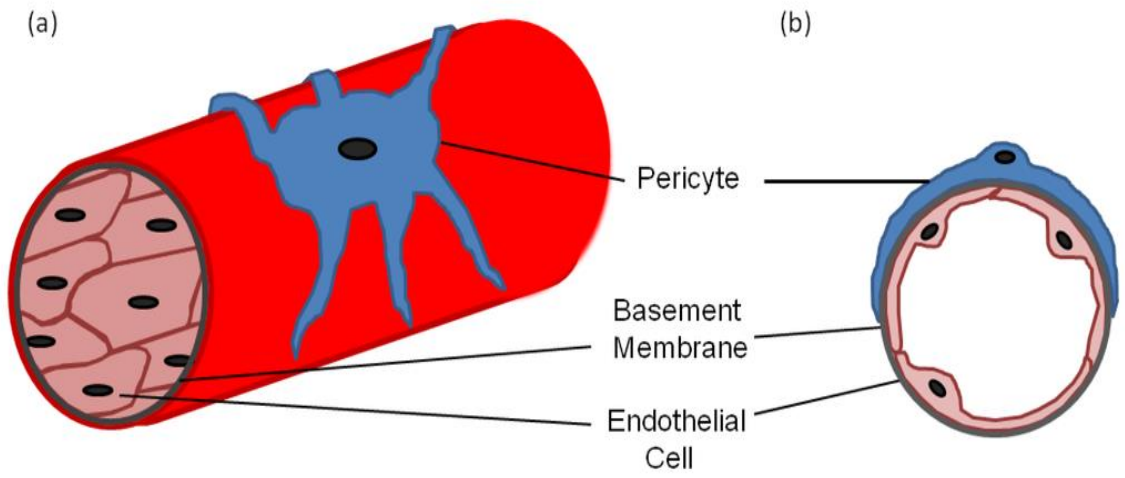

Figure 1: A) A diagram of a blood vessel enwrapped by a pericyte. **B)** A cross-section of a blood vessel demonstrating the interaction between the basement membrane, endothelial cell and a pericyte (Mills, 2013).

B) Resistance Training in Rodents

Skeletal muscle is highly plastic and possesses high capacity to adapt to stresses applied as result of exercise. Exercise-induced adaptation that occurs following resistance exercise includes structural and biochemical changes that promote protection against damage and increased strength in humans (Ogasawara, 2013; Damas, 2015).

There are a number of benefits to using an animal model to study muscle growth following resistance exercise, such as a tight experimental control, a more homogenous sample population and whole-tissue analysis. In addition, the mouse genome can be modified, providing a molecular tool necessary to dissect the biological basis for exercise-induced adaptation. Models of muscle hypertrophy in rodents include: 1) involuntary weighed exercise, 2) compensatory overload, and 3) electrical stimulation models. Involuntary weighted exercise typically involves the attachment of a weighted belt to a rodent and forcing exercise through electrical shock or food deprivation. The greatest advantage of this technique is the direct similarity to human exercise protocols. This model is problematic as it is involuntary and the necessary "motivators" cause stress, resulting in hormonal fluctuations, thereby impacting results. Compensatory overload models focus on inactivation of synergist muscles, thereby rendering the functional muscle to "compensate" for this loss and inducing muscle hypertrophy. Inactivation of synergist muscles is typically attained through severing of a tendon, otherwise known as tenotomy. A complete removal of synergist muscles (synergist ablation) and denervation of synergist muscles are alternate methods to achieve compensatory overload. Chronic overload can lead to extensive muscle growth, providing an efficient model that allows for a better understanding of the hypertrophic mechanism. However, the patterns of neural activation are distinct compared to

traditional resistance exercise and overload can result in extensive damage and inflammation. Thus, this model does not appropriately mimic resistance exercise (Lowe, 2002).

Electrical stimulation is a relatively new model involving the placement of rodents under anesthesia and applying electrical stimuli to the muscle of interest, thereby eliciting muscle contraction. Electrical stimulation was introduced as a novel model for the induction of hypertrophy by Wong and Booth in 1988 and was subsequently replicated by others (Wong, 1988; Baar, 1999; McBride, 2003; McBride, 2006). The advantages of this model include: independence from animal motivation and cooperation, availability of a contralateral control muscle, the ability to create and implement specific exercise protocols, maximal activation of motor units and the ability to quantify the muscle torque during the exercise bout (Lowe, 2002). The downside of this model is the repeated exposure to anesthesia, which may introduce some confounding variables to the results. An illustration of the electrical stimulation is shown in Figure 2.

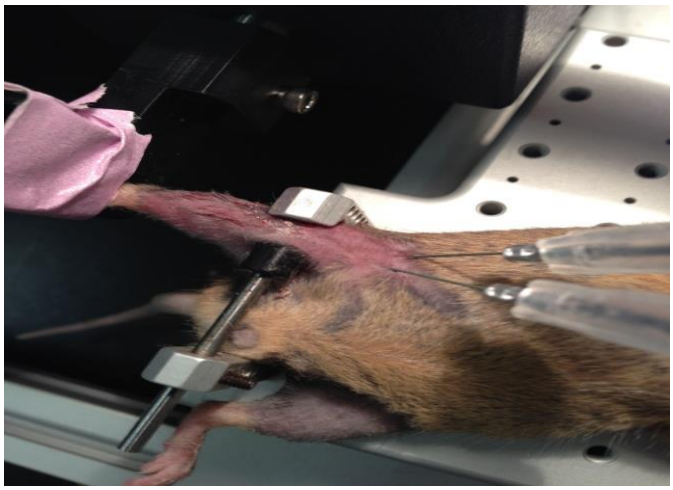

Figure 2: Electrical stimulation of the sciatic nerve as a method to mimic resistance exercise in rodents

C) Electrical Stimulation

Wong & Booth (1988) were the first group to use electrical stimulation to mimic resistance exercise in rodents (Wong, 1988). Their model consisted of electrical stimulation of hindlimbs to contract against a weighed pulley bar for 16 weeks. This protocol resulted in increased gastrocnemius muscle weight and protein content (Wong, 1988). Baar and Esser (1999) used surgical implantation to insert stainless steel electrode wires around the sciatic nerve, then run the wires subcutaneously to the base of the neck, where they were secured and received the electrical stimulation from a stimulation apparatus (Baar, 1999). This protocol resulted in increased extensor digitorum longus (EDL) and tibialis anterior (TA) muscle weight in response to 6 weeks of training (Baar, 1999). Over the past decade, there has been an effort to develop a less intrusive electrical stimulation model for rodents. Low intensity, high volume electrical stimulation demonstrated capacity to increased muscle mass in the medial gastrocnemius, although it did not increase the myofibrillar protein content in rats (Adams, 2003). Two studies by McBride et al. (2003, 2006) demonstrated increases in TA muscle mass and contractile force over a period of 4 weeks (2x/week). Recent work by Ambrosio et al. (2012) and Distefano et al. (2013) utilized surface electrodes to elicit skeletal muscle contractions. Moderate intensity, high volume electrical stimulation applied over 4 weeks produced a large increase in $CD31^+$ vessels (a marker of skeletal muscle vascularity) and an increase in force production in dystrophic mice without any change in muscle mass? (Ambrosio, 2012). Similar results were obtained by a different group using the same exercise protocol in dystrophic mice. Stimulation resulted in increased vascularization and force output, without an increase in muscle CSA, which was attributed to neural adaptation (Distefano, 2013). Moderate intensity electrical stimulation applied over 6 exercise sessions resulted in increases in muscle weight and

myofibrillar protein content, without a change in muscle cross sectional area (CSA) in rats (Tsutaki, 2013). Thus, results among the different studies suggest the potential for electrical stimulation to allow for adaptation, but capacity to induce muscle growth appears to be dependent on the muscle group evaluated and the protocol parameters (inclusion of weighted pulley bar, intensity of stimulus).

D) Pericyte Response to Exercise

Resistance exercise, particularly exercise that includes an eccentric component, can result in skeletal muscle damage. Mechanical strain can directly damage the sarcolemma, disrupt the myofibrillar protein structure within sarcomeres, and degrade proteins necessary for excitation-contraction (E-C) coupling. Together, these disruptions result in a transient, yet significant decrease in force production (Morgan, 2001). Acute damage can initiate a complex series of events that allow for myofiber repair and muscle adaptation. Satellite cells ($Pax7^{+}$), the primary myogenic stem cell for muscle (located between the basal lamina and the sarcolemma), are essential for myofiber repair and regeneration in response to mechanical load-induced injury (McCarthy 2011; Relaix, 2012). Despite the fact that the satellite cell appears to be the only cell type in muscle necessary for repair, the essential factors in the niche necessary for satellite cell activation and differentiation post-exercise remain to be revealed. In addition, the extent to which satellite cells contribute to long-term myofiber hypertrophy post-exercise is also not clear (Fry 2014).

Vascular-associated stem/stromal cells (side population cells, pericytes, mesenchymal progenitors and fibro/adipogenic progenitors) also reside in skeletal muscle and recent studies suggest the ability for these cells to regulate satellite cell proliferation following eccentric exercise (Valero, 2012; Boppart, 2013; Zou, 2015). Previous work in our laboratory focused on a

non-myogenic, mesenchymal progenitor cell population (Sca-1^{+}CD45^{-}) that was observed to accumulate in skeletal muscle in response to an acute bout of eccentric exercise (Valero, 2012). The proportion of Sca-1^{+}CD45^{-} cells increased from 4.3% to 9.4% in wild-type mice at 24h post-exercise. PCR and flow cytometry experiments characterized the cells as negative for Pax7 expression and positive for several pericyte markers (NG2, CD146, PDGFRβ), suggesting heterogeneity of the cell population isolated from muscle (Valero, 2012; Boppart, 2013). The Sca-1^{+}CD45^{-} cells that appear in mouse muscle are primed to secrete an array of growth factors and cytokines, such as IL-6, IGF-1, VEGF, HGF and EGF (Hunstman, 2013; De Lisio, 2014), factors that together may provide the basis for increases in satellite cell quantity, new fiber growth, and vascular growth following an acute bout of eccentric exercise (Valero, 2012; Huntsman, 2013). Additionally, Sca-1^{+}CD45^{-} stromal capacity may be responsible for increases in myofiber growth and muscle strength following repeated bouts of eccentric exercise (Zou, 2015).

Despite compelling data to suggest a role for vascular-associated stem/stromal cells in skeletal muscle repair and adaptation post-exercise, identification of the precise subpopulation responsible for such changes remains elusive due to a lack of unique cell surface markers necessary for detection and isolation. Regardless of the known confounding variable of cell heterogeneity, investigators can use a cell sorting strategy of positive selection for NG2 and CD146 and exclusion of hematopoietic (CD45) and endothelial (CD31) cell markers to isolate a relatively pure pericyte population from muscle (Kostallari, 2015). In addition, CD140A is commonly used to identify mesenchymal stem/stromal or fibroadipogenic progenitors (FAPs) (Joe, 2010; Heredia, 2013). Using these identification strategies, two recent studies demonstrated that pericyte quantity did not change in the acute time course following either isolated concentric

or eccentric contractions (De Lisio 2015) and $NG2^+$ pericyte quantity decreased following 12 weeks of concentric or eccentric training (Farup 2015) in humans. In addition, an increase in proliferating $CD140A^+$ and $CD90^+$ cells was observed in the latter study, suggesting expansion of the MSC population, either as the result of proliferation or a pericyte to MSC transition. Unfortunately, these assessments were based on histological measurements and co-staining for different cell surface markers was limited by extensive background staining. In addition, no information was provided regarding the impact of exercise on pericyte function (gene expression). Thus, the purpose of this project was to thoroughly examine the pericyte response to acute and repeated bouts of resistance exercise in mouse skeletal muscle using multiplex flow cytometry and qPCR methodology.

E) Aims and Hypotheses

The response of vascular-associated stem/stromal cells, such as pericytes, to resistance exercise has not been thoroughly studied. Based on the information provided above, we set out to address the following specific aims:

1. To determine the extent to which pericyte quantity, cell surface marker expression, and gene expression is altered in response to an acute bout of electrical stimulation.
    a. Hypothesis 1: $NG2^{+}CD45^{-}CD31^{-}$ and $CD146^{+}CD45^{-}CD31^{-}$ pericyte quantity will decrease in mouse skeletal muscle following an acute bout of electrical stimulation.
    b. Hypothesis 2: CD140A expression will increase in $NG2^{+}CD45^{-}CD31^{-}$ and $CD146^{+}CD45^{-}CD31^{-}$ pericytes to reflect transition to an MSC phenotype following an acute bout of electrical stimulation.
    c. Hypothesis 3: $NG2^{+}CD45^{-}CD31^{-}$ and $CD146^{+}CD45^{-}CD31^{-}$ pericyte gene expression will be significantly altered following an acute bout of electrical stimulation.
2. To determine the extent to which pericyte quantity and cell surface marker expression is altered in response to repeated bouts of electrical stimulation.
    a. Hypothesis 1: $NG2^{+}CD45^{-}CD31^{-}$ and $CD146^{+}CD45^{-}CD31^{-}$ pericyte quantity will decrease in mouse skeletal muscle following repeated electrical stimulation.
    b. Hypothesis 2: CD140A expression will increase in $NG2^{+}CD45^{-}CD31^{-}$ and $CD146^{+}CD45^{-}CD31^{-}$ pericytes following repeated electrical stimulation.

CHAPTER II

METHODOLOGY

A) Animals

Protocols for animal use were approved by the Institutional Animal Care and Use Committee of the University of Illinois at Urbana-Champaign. Animal experiments in this study were conducted in accordance with the policy statement of the American College of Sports Medicine. 10 week-old male and female C57BL/6J mice were purchased for all of the experiments. All mice were housed in a temperature-controlled animal room maintained on a 12:12 light-dark cycle at the University of Illinois. Mice were fed standard laboratory chow and water *ad libitum*.

B) Electrical Stimulation

C57BL/6J mice were randomly assigned to an electrically stimulated group or a sham operation group. All mice were anesthetized with isoflurane (2-3% isoflurane, 0.9L/min oxygen). Both legs were shaved and aseptically prepared. The mouse foot was placed in a miniature metal foot plate attached to the shaft of a servomotor (model 300 B-LR, Aurora Scientific, Aurora, ON, Canada). The foot was placed so that it was perpendicular to the tibia. Two platinum electrodes were inserted through the skin on either side of the sciatic nerve. A stimulator and stimulus unit activated the sciatic nerve via the platinum electrodes to induce a contraction of the hindlimb crural muscles. The optimal voltage was determined by delivering 100 Hz pulses of 0.1 ms duration and measuring the peak twitch force of each contraction. We tested a range of voltages (50-200Hz) and settled on 100 Hz as this voltage elicited a high peak twitch force that was not further elevated by higher voltages. Additionally, Distefano et al. (2013) demonstrated muscular

strength increase with a relatively low voltage (50 Hz) in dystrophic mice; therefore we did not increase our voltage above 100 Hz. As Distefano et al. (2013) was not able to elicit muscle hypertrophy with this model, we decided to increase the voltage in order to demonstrate muscle growth. The posterior crural muscles performed 20 eccentric and 20 concentric contractions using the optimal voltage at 100 Hz. During stimulation, the posterior crural muscles were stretched from 19° of ankle plantarflexion to 19° of ankle dorsiflexion. Every 5 contractions were separated by 10 second rest periods and the entire protocol lasted 17-21 minutes. The stimulation protocol consisted of 8 sets (4 eccentric and 4 concentric sets). Corona et al. have demonstrated that this electrical stimulation protocol can cause muscle inflammation in mice (Corona, 2010). For this reason, sedentary sham control mice were anesthetized and subjected to electrode insertion, but the muscles were not stimulated.

C) Tissue Collection and Preservation

Twenty-four hours after the final training session, all mice were euthanized via carbon dioxide asphyxiation. Gastrocnemius-soleus muscles were rapidly dissected and were either frozen in liquid nitrogen-cooled isopentane for immunohistochemistry studies or placed in a 1X PBS + penicillin/streptomycin solution for extraction of mononuclear cells.

D) Extraction and Isolation of Vascular-Associated Stem/Stromal Cells

Gastrocnemius-soleus complexes were harvested 24h after the last bout electrical stimulation. The left hindlimb muscle from each mouse was used for mononuclear cell isolation and the right hindlimb muscle was used for immunohistochemistry. Muscles were mechanically disrupted with scissors and then digested in a warm bath (37°C) in a solution of DNAse (Worthington) and Collagenase (Worthington), both diluted at 1:70 in phosphate-buffered saline (PBS). Every 15 minutes the solution was pipetted through a smaller pipette (25ml, 10ml, 5ml, 1ml) for a total digestion time of 1 hour. After enzymatic digestion of the muscle tissue, filtered samples were incubated at 4°C with antimouse CD16/CD32 (1 µg per 106 cells) (eBioscience, San Diego, CA) for 10 minutes to block nonspecific Fc-mediated interactions. Cells were incubated with a cocktail of monoclonal antibodies NG2-FITC (EMD Millipore, Billerica, MA), CD45-APC (BD Bioscience, San Jose, CA), CD31-APC (BD Bioscience, San Jose, CA), CD140a-Pacific Blue (BD Bioscience, San Jose, CA), CD146-PE (Biolegend, San Diego, CA), diluted in 2% fetal bovine serum in PBS. Flow cytometry analysis was performed using a BD LSRFORTESSA X-20 System located at the Digital Computer Laboratory (Urbana, IL). Fluorescence-activated cell sorting was performed using an iCyt Reflection System located at Carle Hospital (Urbana, IL). $CD146^{+}CD45^{-}CD31^{-}$ and $NG2^{+}CD45^{-}CD31^{-}$ cells were collected in tubes with RLT buffer and frozen at -80°C for gene expression. For both flow cytometry and FACS experiments, negative and single-stained controls were used to establish gates and perform compensation.

E) Gene Expression

RNA isolation and cDNA synthesis. RNA was extracted from cell lysates using RNeasy Micro Kit (Qiagen), following the manufacturer's instruction. Quantity and quality of isolated RNA was assessed in duplicate on a Take-3 application plate using a Synergy H1 Hybrid Multi-Mode Microplate Reader (BioTek, Winooski, VT). Starting RNA concentration of at least 15ng was used to perform reverse transcription via the High Capacity cDNA Reverse Transcription Kit (Life Technologies, Grand Island, NY) per manufacturer's instructions.

cDNA preamplification and quantitative PCR. Preamplification of cDNA was completed using TaqMan PreAmp Master Mix Kit (Life Technologies). The primer pool was composed of inventoried Taqman primers, which were diluted in Tris-EDTA buffer to a final concentration of 0.2x. In a thin-walled 0.2mL PCR tube, PreAmp reagent was mixed with the primer pool and sample cDNA. Each reaction was amplified for 14 cycles using a thermo-cycler (ABI Geneamp 9700, Life Technologies). Samples were diluted in 450-900 μL of diethylpyrocarbonate (DEPC) RNase-free water. qPCR was performed using the 7900HT Fast Real-Time PCR System with Taqman Universal PCR Master Mix (Applied Biosystems, Grand Island, NY). All genes were normalized to hypoxanthine guanine phosphoibosyl transferase (HPRT) or glyceraldahyde-3-phosphate dehydrogenase (GAPDH), and expressed relative to corresponding control condition. Gene expression data is presented using the ΔΔCT method with cycle threshold (Ct) replicate values within 0.5 Ct units. Inventoried Taqman primers were purchased from Applied Biosystems. Primer information and gene expression assay ID numbers used in this study are provided in the appendix: experimental protocols.

F) Immunohistochemistry

Muscle complexes were cut at the midline along the axial plane. The distal end was embedded in an optimum cutting temperature compound (Tissue-Tek; Fischer Scientific). Three transverse cryosections per sample (10-µm nonserial sections, each separated by a minimum of 40 µm) were cut for each histological assessment using a CM3050S cryostat (Lecia, Wezlar, Germany). Sections were placed on microscope slides (Superfrost; Fischer Scientific, Hanover Park, IL) and stored at -80°C before staining. Sections were stained with antibodies against mouse IgG2b monoclonal anti-type 1 MHC (clone BA-D5, 1:20), mouse IgG1 monoclonal anti-type 2a MHC (clone SC-71, 1:50), mouse IgM monoclonal anti-type 2b MHC (clone BF-F3, 1:50) and mouse IgM monoclonal anti-type 2x MHC (clone 6H1, 1:20) to determine the fiber-type specific cross sectional area (CSA).

Briefly, slides were dried and fixed in acetone for 10 minutes followed by several washes in 1X PBS. Sections were then blocked with serum for 1 hour and incubated with 1:10 dilution of goat antimouse monovalent Fab fragments (AffiniPure Fab Fragment Goat Anti-Mouse IgG (H+L); Jackson Immuno-Research Laboratories, Inc., West Grove, PA). After blocking, sections were incubated in the primary antibodies for 1 hour at room temperature (Fiber-Type Specific staining, IgG). After several washes with 1X PBS (Fiber-Type Specific staining), sections were incubated in the appropriate secondary antibodies for 1 hour at room temperature. IgG antibody was applied to tissue sections at 4°C overnight. Sections were washed with 1X PBS (Fiber-Type Specific staining) and with 1% BSA/stained with 4´,6-diamidino-2-phenylindole (DAPI, 1:20,000; Sigma-Aldrich, St. Louis, MO) (IgG) before mounting with Vectashield (Vector Laboratories).

G) Immunohistochemistry Quantification

To assess myofiber CSA, Adobe Photoshop was used to quantitate images acquired with a Zeiss AxioCam digital camera. Briefly, co-stained images of dystrophin and type-specific fiber types were acquired at 10X magnification from each sample, then imported into Adobe Photoshop (CS5 Extended) where up to 400 fibers per sample were manually circled using the magnetic lasso tool, which grabs the positively stained pixels and decreases subjectivity and interassessment error. The CSA for each fiber was recorded in a measurement log. The results for each sample were then averaged.

H) Statistical Analysis

All averaged data are presented as means ±SEM. To determine significance, comparisons between groups were evaluated by either T-test (acute and chronic electrical stimulation flow cytometry) or two-way ANOVA followed by the LSD post-hoc tests when significant interactions were detected (acute electrical stimulation gene expression). Data was considered significant at $p \leq 0.05$. All calculations were performed with GraphPad Prism statistical software (6.0; GraphPad Software, San Diego, CA).

I) List of Materials

Material	Company	Product #
Anti-Mouse CD16/CD32	eBioscience	14-0161-81
Anti-Dystrophin	abcam	Ab15277
APC Rat Anti-Mouse CD45	BD	559864
APC Rat Anti-Mouse CD31	BD	551262
PE anti-mouse CD146 Antibody	BD	134703
BV421 Rat Anti-Mouse CD140A	BD	562774
Anti-NG2, Alexa Fluor®488 Conjugate Antibody	Millipore	AB5320A4
Dispase	Worthington	LS02104
Collagenase	Worthington	LS004174
Mouse IgM anti-type 2b MHC	Developmental Studies Hybridoma Bank	BF-F3
Mouse IgG1 anti-type 2a MHC	Developmental Studies Hybridoma Bank	SC-71
Mouse IgG2b anti-type I MHC	Developmental Studies Hybridoma Bank	BA-D5
Mouse IgM anti-type 2x MHC antibody	Developmental Studies Hybridoma Bank	6H1
Goat anti-Mouse IgG2b Secondary Antibody, Alexa Fluor® 350 conjugate	Life Technologies	A-21140
AMCA AffiniPure Goat Anti-Mouse IgM, µ Chain Specific	Jackson ImmunoResearch	115-155-075
Alexa Fluor® 488 AffiniPure Goat Anti-Mouse IgM, µ Chain Specific	Jackson ImmunoResearch	115-545-075
Alexa Fluor® 488 AffiniPure Goat Anti-Mouse IgG, Fcγ Subclass 1 Specific	Jackson ImmunoResearch	115-545-205
High Capacity cDNA Reverse Transcription Kit	Life Technologies	4368814
Taqman Universal PCR Master Mix	Applied Biosystems	4304437

J) Experimental Design

1) Acute Electrical Stimulation (Flow Cytometry)

The purpose of this experiment was to determine the extent to which an acute bout of electrical stimulation can alter pericyte quantity and cell surface marker expression. Seventeen week-old C57BL/6 WT mice (n=5, all males) were subjected to bilateral electrical stimulation. Age-matched sham mice (n=4) received the same amount of anesthesia and bilateral electrode insertion, without application of electrical stimulation. Due to shipment delays of digestion enzymes necessary for cell isolation, this cohort of mice is older than 10 week-old animals used in other experiments. Muscles were collected 24h post-intervention.

2) Acute Electrical Stimulation (Gene Expression)

The purpose of this experiment was to determine the extent to which an acute bout of electrical stimulation can alter pericytes gene expression. Ten week-old male and female C57BL/6 WT mice (n=4; 2 males and 2 females) were subjected to bilateral electrical stimulation. Age-matched shams (n=4; 2 males and 2 females) received the same amount of anesthesia and bilateral electrode insertion, without application of electrical stimulation. Muscles were collected 24h post-intervention.

3) Repeated Electrical Stimulation

The purpose of this experiment was to determine the extent to which repeated bouts of electrical stimulation can alter pericyte quantity and cell surface marker expression. Ten week-old C57BL/6 WT mice were electrically stimulated twice weekly for 4 weeks (n=8; 4 males and 4 females) or 9 weeks (n=6; 3 males and 3 females). For the 4 week study, age-matched shams (n=4; 2 males and 2 females) received the same amount of anesthesia and bilateral electrode

insertion, without application of electrical stimulation. The 9 week study is a report of preliminary data collected to verify our model. Two age-matched shams were included. For both training studies, muscles were collected 24h post-intervention. One muscle was used for assessment of histology and the other muscle was used for assessment of cell quantity and cell surface marker expression by flow cytometry.

CHAPTER III

RESULTS

A) Flow Cytometry Analysis of the Skeletal Muscle Response to Acute Electrical Stimulation

Figure 3 illustrates the gating of various mononuclear cell populations in skeletal muscle following an acute bout of electrical stimulation. Two subpopulations were noted for $CD146^+$ cells, including one population that exhibited low expression and another that exhibited high expression (Figure 3F). The total percentage of $NG2^+$, $CD146^+$, Lin^+ (CD45 and CD31), and $CD140A^+$ mononuclear cells did not change in skeletal muscle 24h following a single bout of electrical stimulation (Figures 4A-D).

Upon exclusion of the Lin^+ fraction, a non-significant trend toward an increase in $NG2^+$ ($p=0.1238$) and $CD146^+$ ($p=0.0658$) pericytes was observed following stimulation compared to sham controls (Figures 4E-F). Exclusion of the Lin^+ fraction did not significantly alter the relative percentage of $NG2^+$ or $CD146^+$ cells, as the percentage remained steady in the sham groups at ~5% for $NG2^+$ cells and 50-56% for $CD146^+$ cells. CD140A is a common mesenchymal stem/stromal cell marker (MSC) and we used it to test our hypothesis of pericyte to MSC transition. Interestingly, the percentage of $NG2^+Lin^-$ cells expressing CD140A increased in response to stimulation ($p<0.01$ vs. sham; 22% to 48 %) (Figure 5A). Nearly 80% of the $CD146^+Lin^-$ fraction expressed CD140A in the sham group, suggesting alignment of this pericyte fraction with MSCs. Despite the baseline elevation, a strong trend toward an increase in CD140A expression was still noted in the $CD146^+Lin^-$ fraction post-exercise ($p=0.0550$ vs. sham) (Figure 5B). CD146 expression was observed in only ~10% of the $NG2^+Lin^-$ fraction and did not significantly increase 24h post-stimulation (Figure 5C).

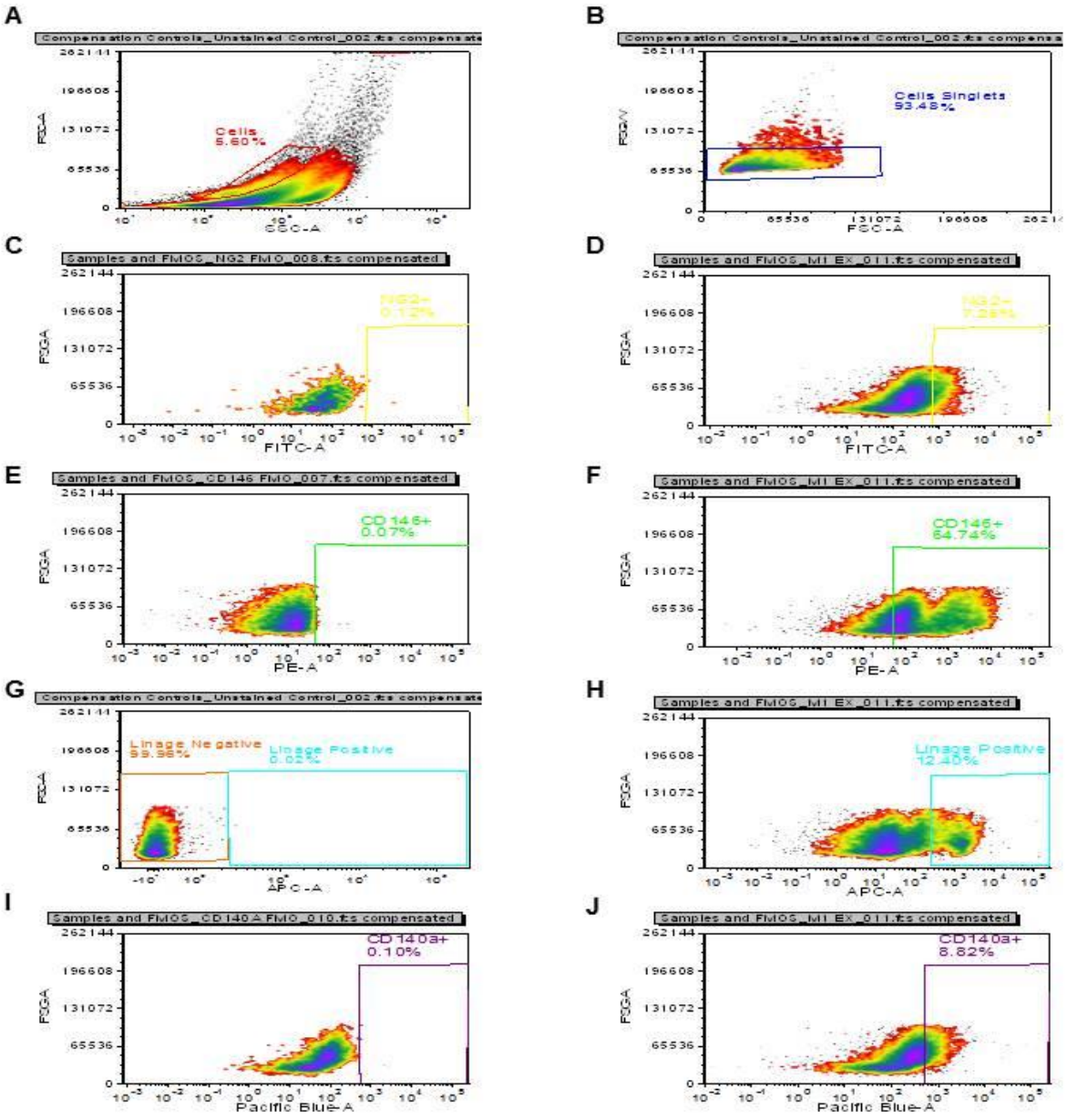

Figure 3 Flow cytometry gating. Population of interest **(A)** and elimination of doublets **(B)**, $NG2^+$ FMO **(C)** and a representative image of the $NG2^+$ population in an electrically-stimulated mouse **(D)**, $CD146^+$ FMO **(E)** and a representative image of the $CD146^+$ population in an electrically-stimulated mouse **(F),** $CD45^+CD31^+$ FMO **(G)** and a representative image of the $CD45^+CD31^+$ population in an electrically-stimulated mouse **(H),** $CD140A^+$ FMO **(I)** and a representative image of the $CD140A^+$ population in an electrically-stimulated mouse **(J)**.

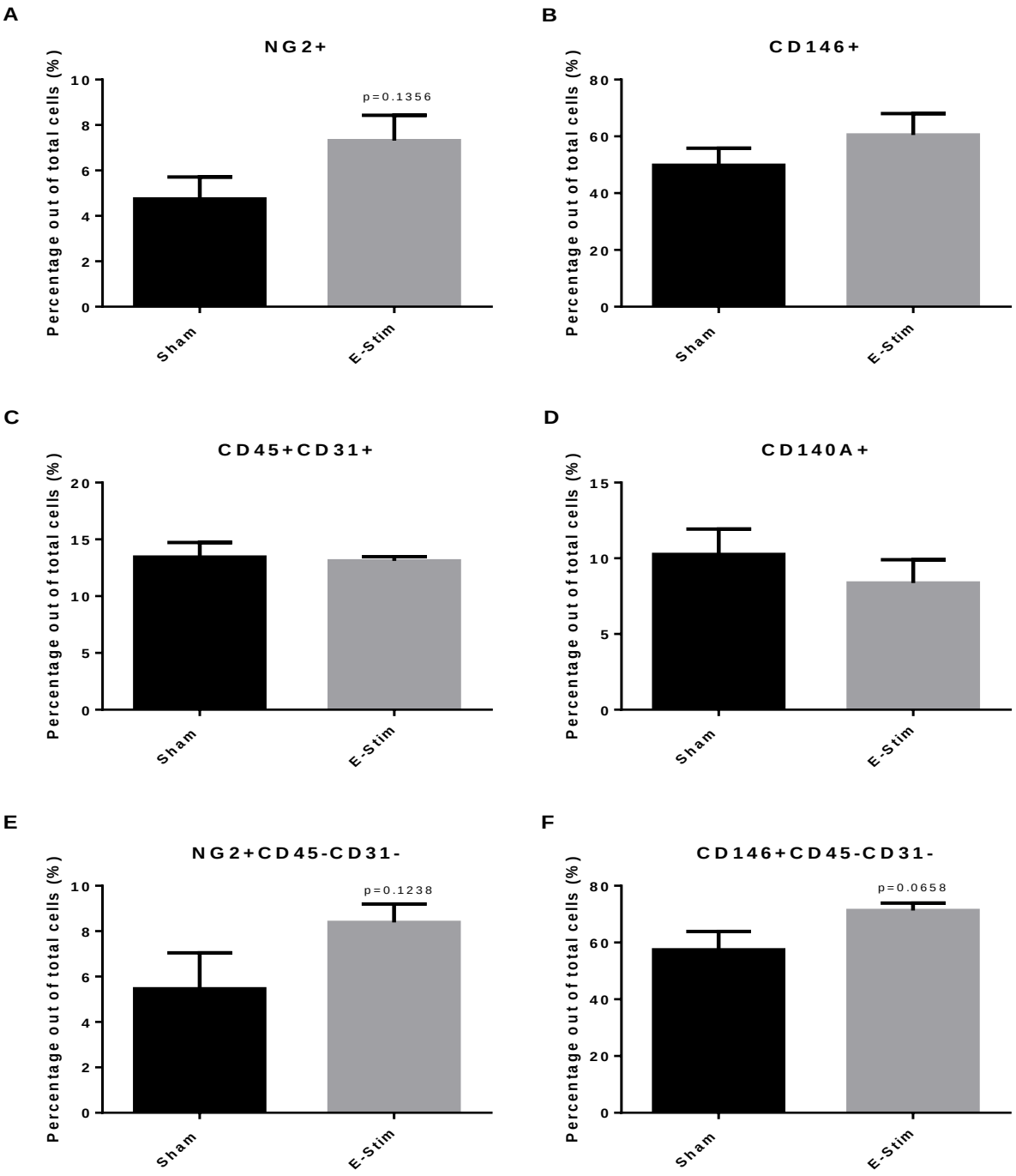

Figure 4 Flow cytometry analysis of mononuclear cells in skeletal muscle following an acute bout of electrical stimulation. Nine 17 week-old mice were subjected to a single bout of electrical stimulation. Gastrocnemius-soleus complexes were harvested and processed 24h post-exercise. $NG2^{+}$**(A)**, $CD146^{+}$**(B)**, $CD45^{+}CD31^{+}$**(C)**, $CD140A^{+}$**(D)**, $NG2^{+}CD45^{-}CD31^{-}$**(E)**, and $CD146^{+}CD45^{-}CD31^{-}$**(F)** response to acute electrical stimulation. Values are mean ± SEM. n = 4-5 muscles/group.

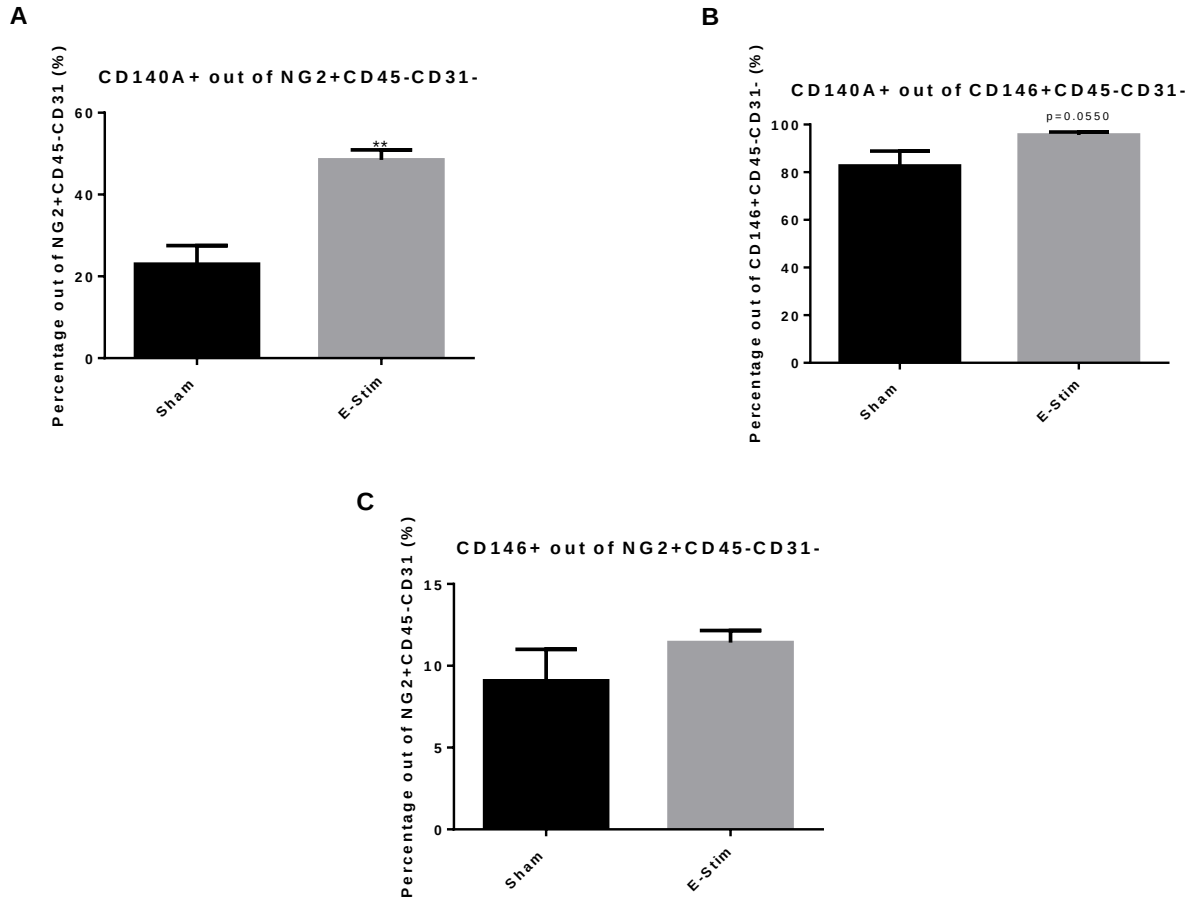

Figure 5 Evaluation of cell surface marker expression in skeletal muscle pericytes following an acute bout of electrical stimulation. Mice were subjected to a single bout of electrical stimulation and gastrocnemius-soleus complexes were harvested and processed at 24h. $CD140A^+$ percentage out of $NG2^+CD45^-CD31^-$ pericytes **(A)**, $CD140A^+$ percentage out of $CD146^+CD45^-CD31^-$ pericytes **(B)** and $CD146^+$ percentage out of $NG2^+CD45^-CD31^-$ pericytes **(C)**. Values are mean ± SEM. n = 4-5 muscles/group; **p<0.01 vs. sham.

B) Gene Expression of Skeletal Muscle Pericytes in Response to Acute Electrical Stimulation

We initially isolated $NG2^{+}CD45^{-}CD31^{-}$ pericytes from skeletal muscle following an acute bout of electrical stimulation. Although cells were viable and high quality RNA was obtained, CT values were very high. Therefore, the $CD146^{+}CD45^{-}CD31^{-}$ pericyte population was evaluated given its high abundance in skeletal muscle. High throughput qPCR included assessment of genes involved in myogenesis (Figure 6), myofiber repair (Figure 7), nerve repair/neurogenesis (Figure 8), extracellular matrix (ECM) remodeling (Figure 9), and inflammation (Figure 10).

Whereas MyoD relative mRNA expression was not significantly altered (Figures 6A-B), Myf5 relative mRNA expression was significantly increased in response to acute electrical stimulation ($p<0.05$ vs. sham) (Figure 6C), and this increase was only evident in female mice ($p<0.01$ vs. female sham) (Figure 6D).

Leukemia inhibitory factor (Lif) relative mRNA expression was significantly increased in response to electrical stimulation ($p<0.05$ vs. sham) (Figure 7A), whereas hepatocyte growth factor (Hgf) relative mRNA expression was not statistically significant in the combined sex analysis (Figure 7B). Non-significant trends toward an increase in Lif and Hgf gene expression were noted only in females (Lif: $p=0.0860$ vs. female sham, Hgf: 0.0790 vs. female sham) (Figure 7B and 7D). Insulin-like growth factor (Igf-1) was significantly elevated in response to exercise ($p<0.01$ vs. sham). Non-significant trends toward an increase in Igf-1 expression was noted in both male ($p=0.0748$) and female ($p=0.0635$) mice (Figures 7E-F). Vascular endothelial growth factor (Vegfa) relative mRNA expression was not changed in response to electrical stimulation (Figures 7G-H).

Brain-derived neurotrophic factor (Bdnf), nerve growth factor (Ngf), and neurotrophin-3 (Ntf3) gene expression was not altered in response to an acute bout of electrical stimulation (Figures 8A-F). Fibronectin type III domain-containing protein 5 (Fndc5) gene expression trended towards an increase in the exercised group compared to sham, and a trend for increase was observed in females ($p=0.0614$ vs. female sham) (Figures 8G-H).

TIMP metallopeptidase inhibitor 2 (Timp2) and matrix metalloproteinase 9 (Mmp9) gene expression was not significantly altered in response to electrical stimulation (Figures 9C-D, G-H). Timp1 was significantly upregulated in response to exercise ($p<0.05$ vs. sham) and a significant increase was observed in males ($p<0.05$ vs. male sham) (Figures 9A-B). Mmp2 and Mmp14 was significantly increased in response to an acute bout of electrical stimulation ($p<0.01$ vs. sham) (Figures 9C-D, I-J).

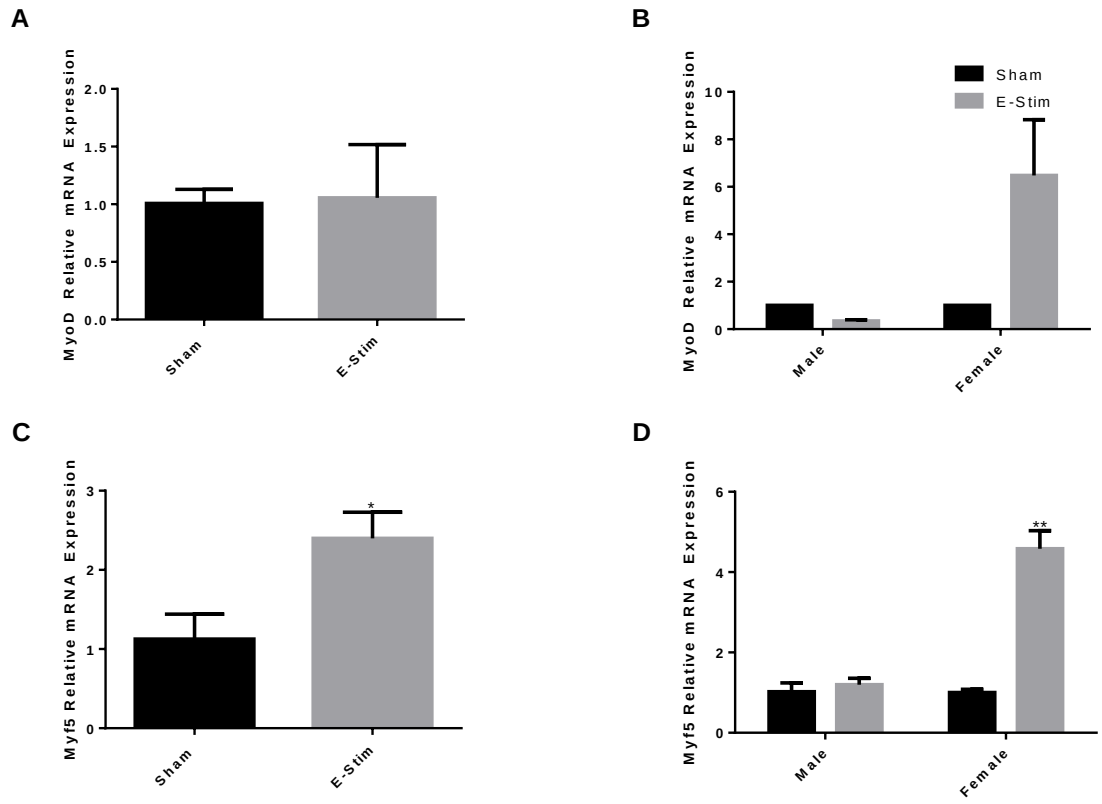

Figure 6 CD146^{+}CD45^{-}CD31^{-} Pericyte myogenic factor gene expression following an acute bout of electrical stimulation. Eight 10 week-old mice were subjected to a single bout of electrical stimulation. Gastrocnemius-soleus complexes were harvested and processed 24h post electrical stimulation. Combined **(A)** and sex-specific **(B)** MyoD relative mRNA expression, combined **(C)** and sex-specific **(D)** Myf5 relative mRNA expression in response to acute electrical stimulation. Values are mean ± SEM. n = 2(B,D) and n=4(A,C) muscles/group; *p<0.05 vs. sham; **p<0.01 vs. sham.

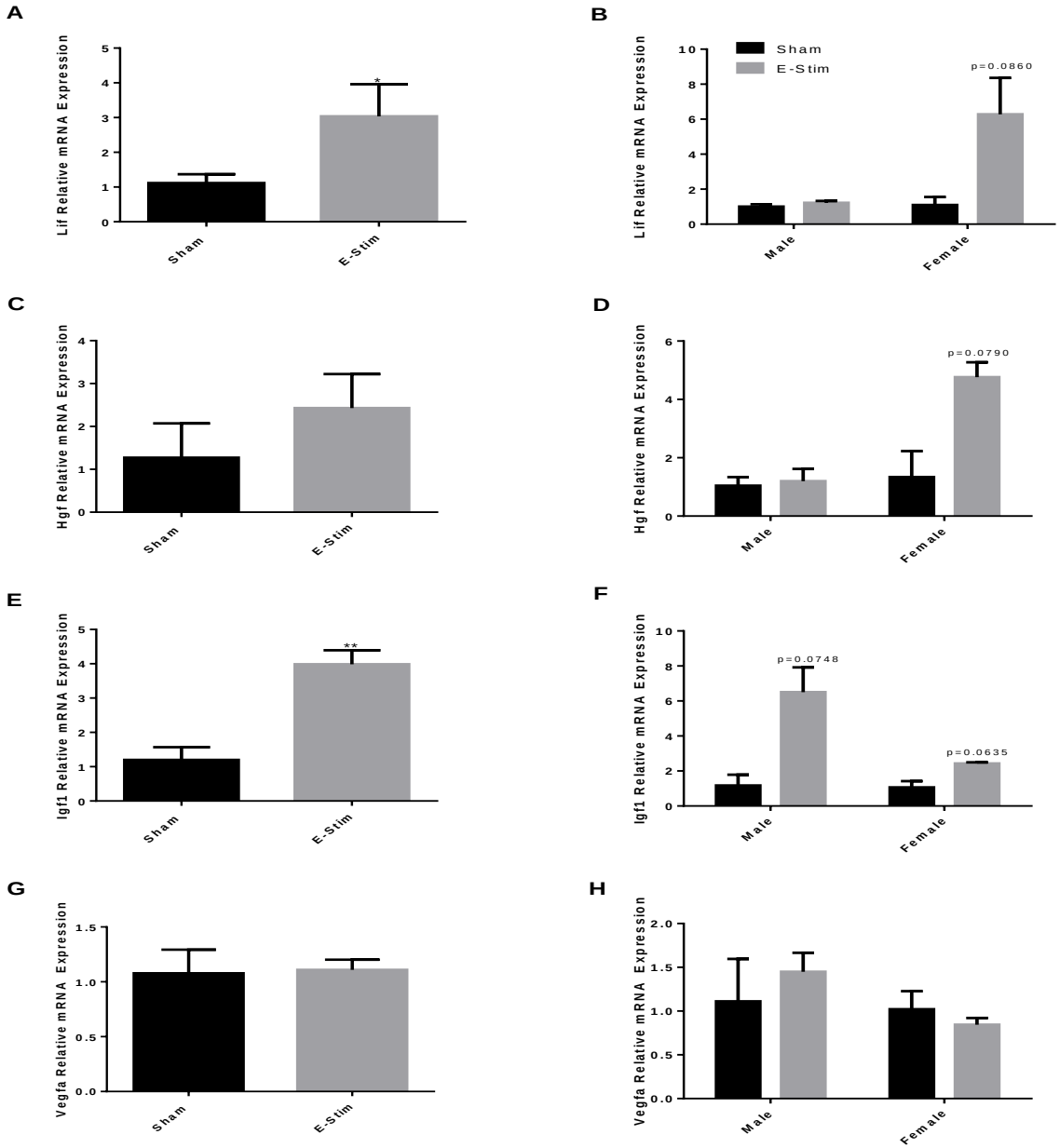

Figure 7 CD146^{+}CD45^{-}CD31^{-} Pericyte growth factor gene expression following an acute bout of electrical stimulation. Eight 10 week-old mice were subjected to a single bout of electrical stimulation. Gastrocnemius-soleus complexes were harvested and processed 24h post electrical stimulation. Combined **(A)** and sex-specific **(B)** Lif relative mRNA expression, combined **(C)** and sex-specific **(D)** Hgf relative mRNA expression, combined **(E)** and sex-specific **(F)** Igf1 relative mRNA expression, combined **(G)** and sex-specific **(H)** Vegfa relative mRNA expression in response to acute electrical stimulation. Values are mean ± SEM. n = 2(B,D,F,H) and n=4(A,C,E,G) muscles/group; *p<0.05 vs. sham; **p<0.01 vs. sham.

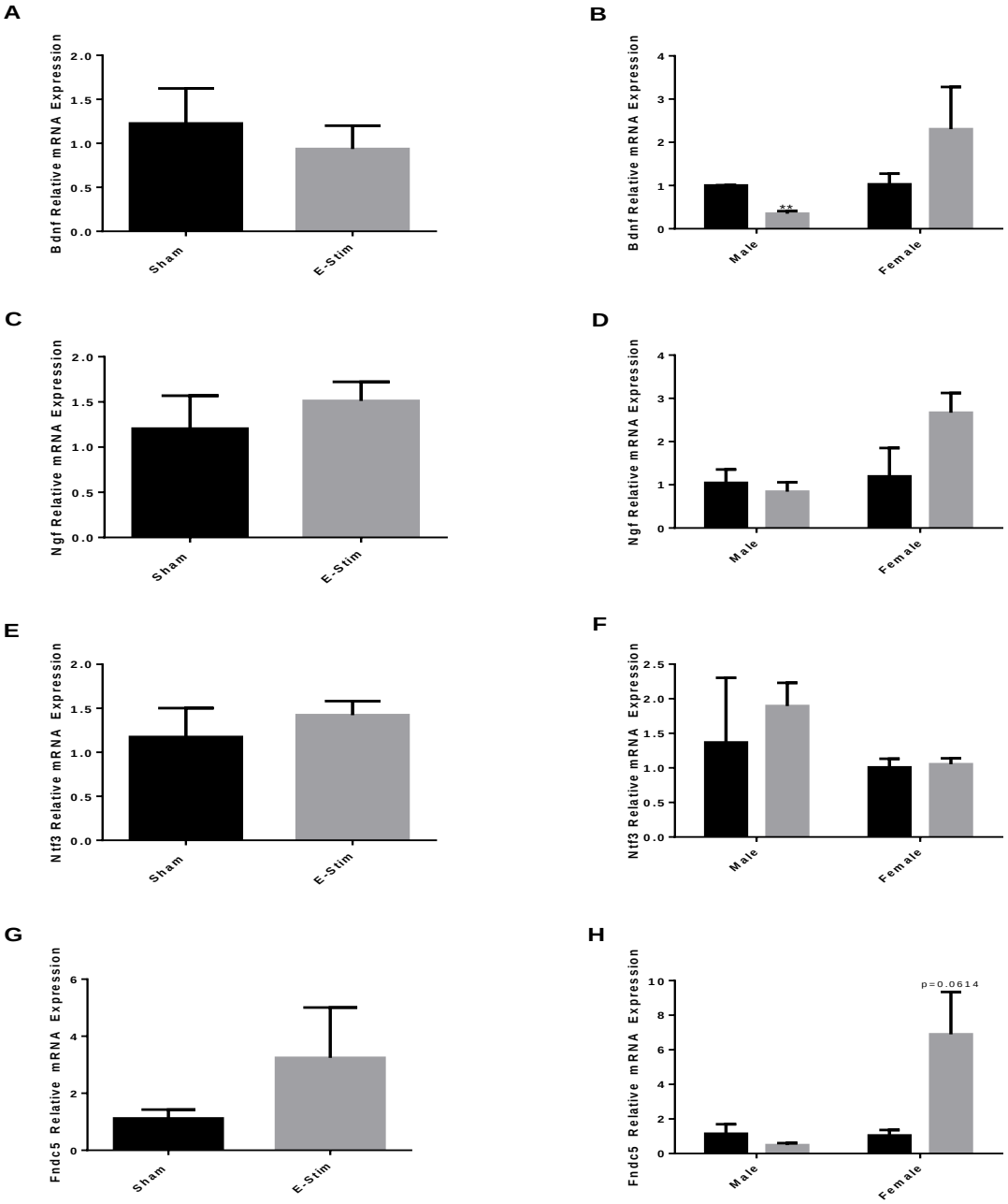

Figure 8 CD146^{+}CD45^{-}CD31^{-} Pericyte neurotrophic factor gene expression following an acute bout of electrical stimulation. Eight 10 week-old mice were subjected to a single bout of electrical stimulation. Gastrocnemius-soleus complexes were harvested and processed 24h post electrical stimulation. Combined **(A)** and sex-specific **(B)** Bdnf relative mRNA expression, combined **(C)** and sex-specific **(D)** Ngf relative mRNA expression, combined **(E)** and sex-specific **(F)** Ntf3 relative mRNA expression, combined **(G)** and sex-specific **(H)** Fndc5 relative mRNA expression in response to acute electrical stimulation. Values are mean ± SEM. n = 2(B,D,F,H) and n=4(A,C,E,G) muscles/group; **p<0.01 vs. sham.

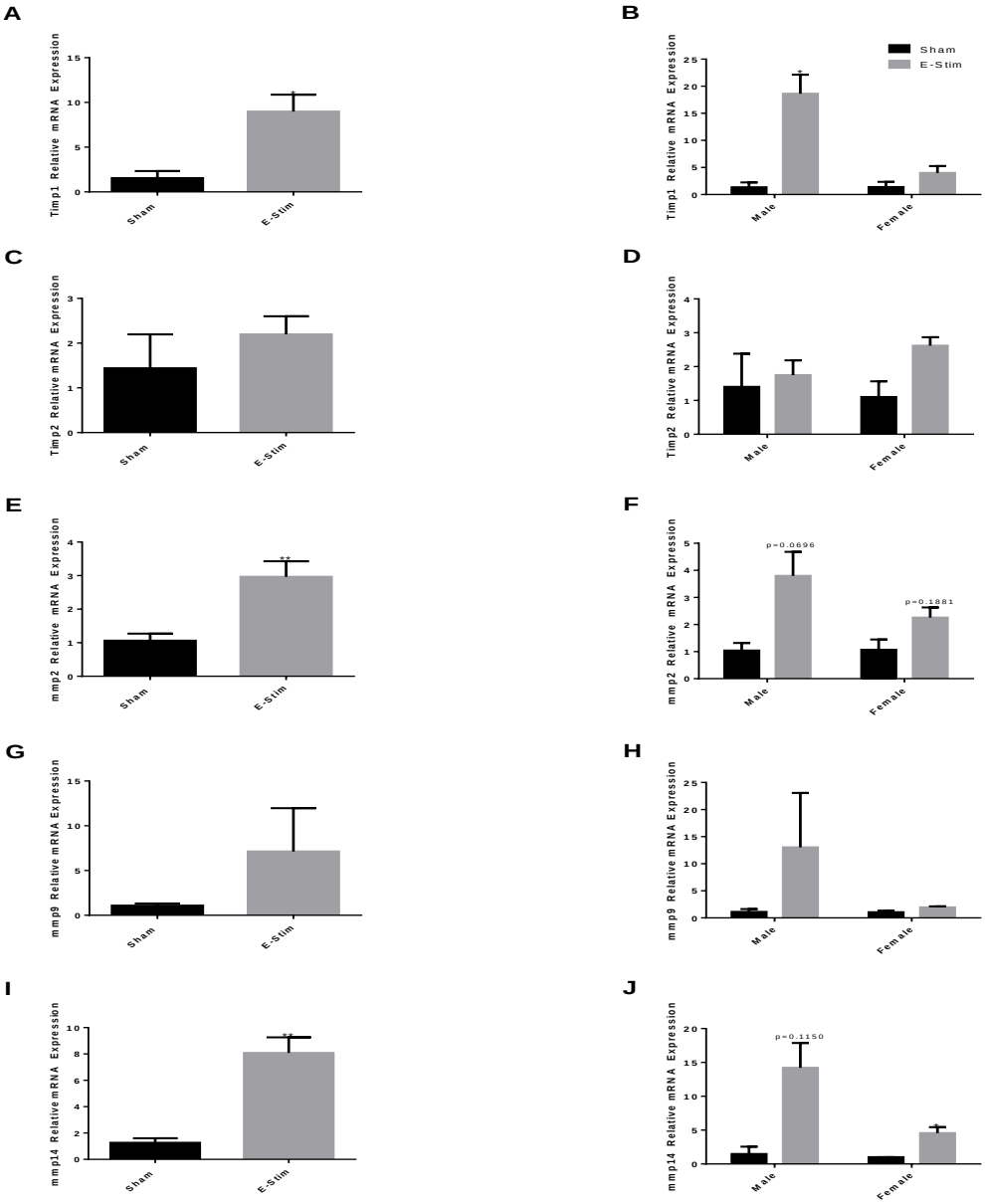

Figure 9 CD146^{+}CD45^{-}CD31^{-} Pericyte extracellular matrix marker gene expression following an acute bout of electrical stimulation. Eight 10 week-old were subjected to a single bout of electrical stimulation. Gastrocnemius-soleus complexes were harvested and processed 24h post electrical stimulation. Combined **(A)** and sex-specific **(B)** Timp1 relative mRNA expression, combined **(C)** and sex-specific **(D)** Timp2 relative mRNA expression, combined **(E)** and sex-specific **(F)** Mmp2 relative mRNA expression, combined **(G)** and sex-specific **(H)** Mmp9 relative mRNA expression, combined **(I)** and sex-specific **(J)** Mmp14 relative mRNA expression in response to acute electrical stimulation. Values are mean ± SEM. n = 2(B,D,F,H,J) and n=4(A,C,E,G,I) muscles/group; *p<0.05 vs. sham; **p<0.01 vs. sham.

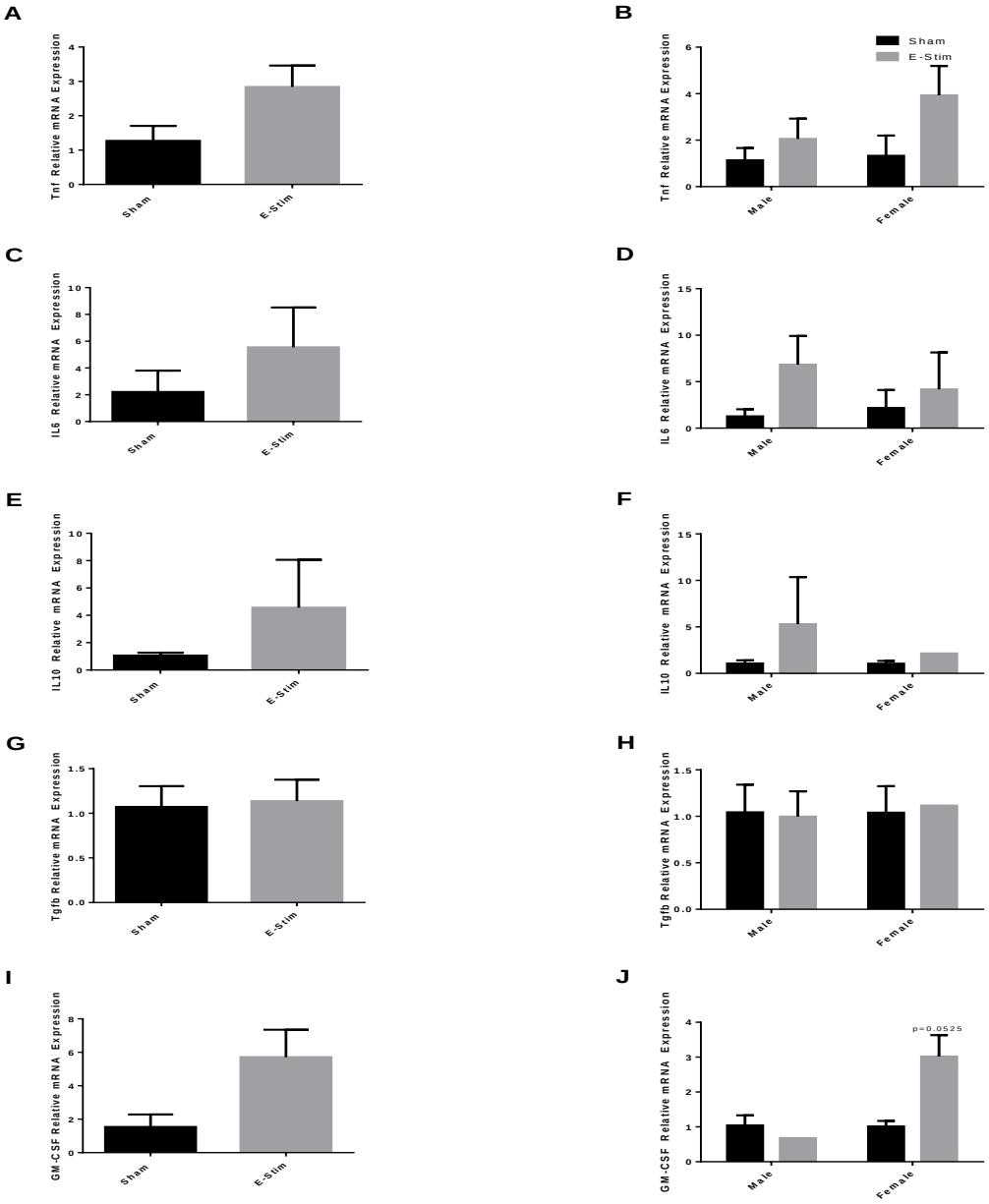

Figure 10 CD146^{+}CD45^{-}CD31^{-} Pericyte cytokine gene expression following an acute bout of electrical stimulation. Eight 10 week-old mice were subjected to a single bout of electrical stimulation. Gastrocnemius-soleus complexes were harvested and processed 24h post electrical stimulation. Combined **(A)** and sex-specific **(B)** Tnf relative mRNA expression, combined **(C)** and sex-specific **(D)** IL6 relative mRNA expression, combined **(E)** and sex-specific **(F)** IL10 relative mRNA expression, combined **(G)** and sex-specific **(H)** Tgfb relative mRNA expression, combined **(I)** and sex-specific **(J)** GM-CSF relative mRNA expression in response to acute electrical stimulation. Values are mean ± SEM. n = 2(B,D,F,H,J) and n=4(A,C,E,G,I) muscles/group.

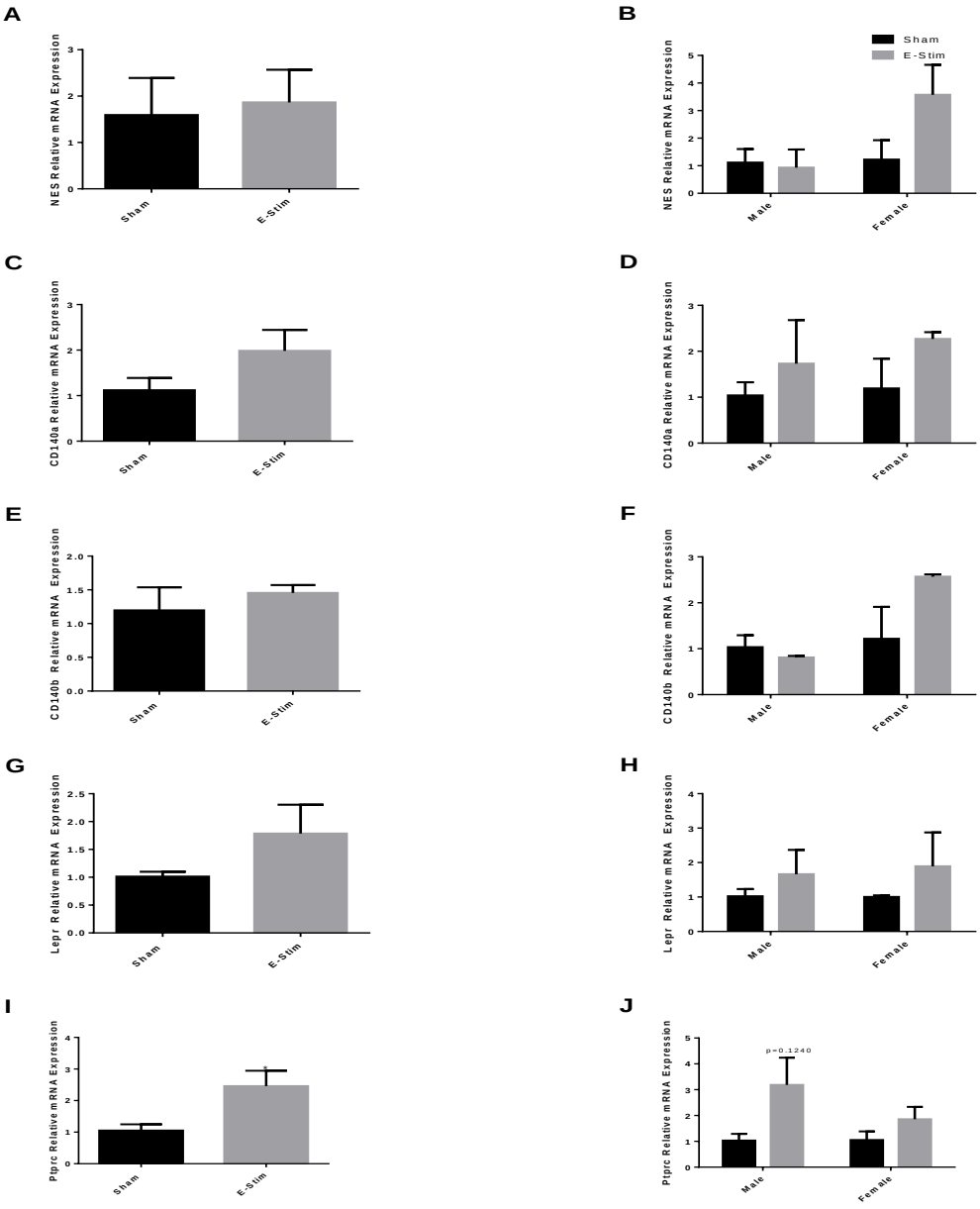

Figure 11 CD146^{+}CD45^{-}CD31^{-} Pericyte mononuclear cell gene expression following an acute bout of electrical stimulation. Eight 10 week-old mice were subjected to a single bout of electrical stimulation. Gastrocnemius-soleus complexes were harvested and processed 24h post electrical stimulation. Combined **(A)** and sex-specific **(B)** NES relative mRNA expression, combined **(C)** and sex-specific **(D)** CD140A relative mRNA expression, combined **(E)** and sex-specific **(F)** CD140B relative mRNA expression, combined **(G)** and sex-specific **(H)** Lepr relative mRNA expression, combined **(I)** and sex-specific **(J)** Ptprc relative mRNA expression in response to acute electrical stimulation. Values are mean ± SEM. n = 2(B,D,F,H,J) and n=4(A,C,E,G,I) muscles/group; *p<0.05 vs. sham.

Both tumor necrosis factor alpha (Tnf) and interleukin 6 (IL-6) demonstrated a trend for increase with electrical stimulation, but were not significant (Figures 10A-D). IL-10 also demonstrated a male-driven trend for increase in response to electrical stimulation, but it was not significant (Figures 10E-F). Transforming growth factor beta (Tgfb) gene expression was not altered and granulocyte macrophage colony-stimulating factor (GM-CSF) gene expression trended towards a female-driven increase in the electrical stimulation group (Figures 10G-J).

Lastly, we were interested in examining stem/stromal marker gene expression following electrical stimulation. Both nestin (NE) and beta-type platelet-derived growth factor receptor (CD140B) gene expression was not altered in response to electrical stimulation (Figures 11A-B, E-F). CD140A and leptin receptor (Lepr) remained unchanged compared to the sham group (Figures 11C-D, G-H). Interestingly, protein tyrosine phosphatase receptor type, C (Ptprc, also known as CD45) relative mRNA expression was significantly increased in response to acute electrical stimulation ($p<0.05$ vs. sham) (Figures 11I-J).

C) Skeletal Muscle Response to Chronic Electrical Stimulation

The chronic electrical stimulation study consisted of two cohorts: 8 mice exercised for 4 weeks and 6 mice exercised for 9 weeks (Figure 12A). One of the goals with this experiment was to determine the validity of our electrical stimulation model by examining the muscular strength and muscular growth responses to chronic training. Body weights were not significantly changed in response to chronic electrical stimulation (Figure 12B-C). We observed a higher average muscle weight in males in response to 4 weeks of electrical stimulation (sex main effect $p<0.0001$) (Figure 12D), but this sex difference was not present at 9 weeks (Figure 12E).

Our electrical stimulation model system allowed us to record the torque achieved during each contraction. As eccentric contractions produce higher force compared to concentric contractions, we decided to record the torque of the first and last eccentric contractions. Peak torque generated during first eccentric contraction reflects capacity for force generation and strength, whereas peak torque generated during the last contraction provides information regarding fatigue resistance. While peak torque of the first contraction was elevated in the males compared to females (sex main effect, $p=0.0016$), no increase was observed as a result of repeated electrical stimulation (e-stim main effect $p=0.1202$) (Figure 13A). In addition, no increase in peak force was observed during the first contraction after 9 weeks of electrical stimulation (Figure 13B). In contrast, peak torque of the last contraction significantly increased after 4 weeks of exercise in both males and females (e-stim main effect $p=0.0003$) (Figure 13C) and the elevation in peak torque during the last bout of contraction was also observed after 9 weeks of electrical stimulation (e-stim main effect $p=0.0173$) (Figure 13D).

Fiber type-specific changes in CSA were evaluated by standard immunohistochemistry methods. The CSA of type 2a, type 2b and type 2x fibers did not change compared to sham after chronic electrical stimulation (Figures 14A-B). Next, we decided to examine the fiber size distribution of these fibers, but only type 2b fibers underwent significant changes in response to 9 weeks of electrical stimulation (Figures 14C-H). Large (2000-3000) type 2b fibers increased ($p<0.05$ vs. sham) in size, but the largest (3000+) type 2b fibers decreased ($p<0.01$ vs. sham) after 9 weeks of repeated stimulation.

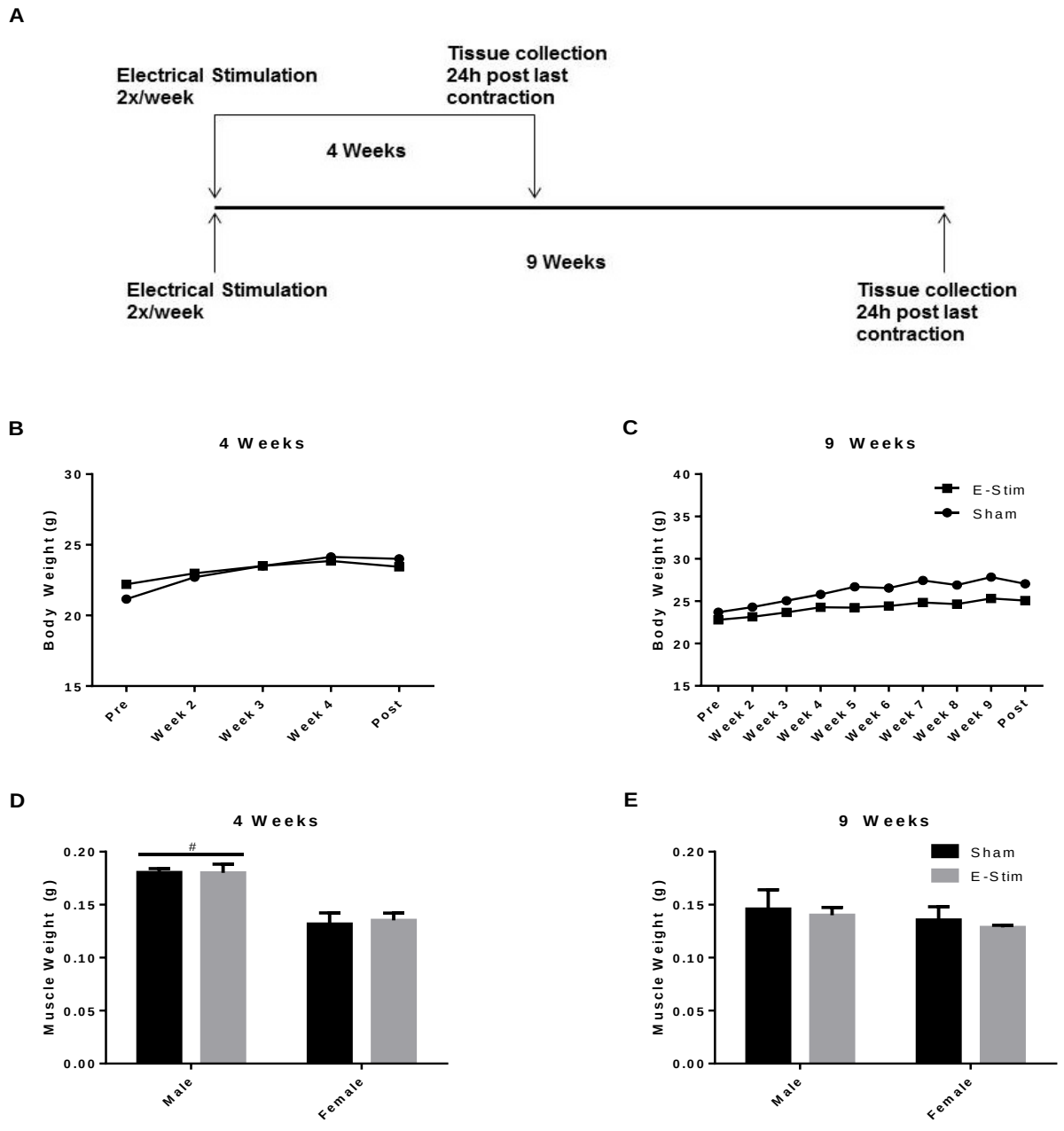

Figure 12 Body weights and muscle weights in response to 4 and 9 weeks of electrical stimulation. Eight 10 week-old mice were subjected to 4 weeks of electrical stimulation twice weekly and six 10 week-old mice were subjected to 9 weeks of electrical stimulation twice weekly. Gastrocnemius-soleus complexes were harvested and processed 24h after the last electrical stimulation bout. Experimental design **(A)**, body weight progression at 4 weeks **(B)** and 9 weeks **(C)**, muscle weights after training at 4 weeks **(D)** and 9 weeks **(E)**. Values are mean ± SEM. n = 2 (9 week shams) and n = 4 (4 week shams/e-stim, 9 week e-stim) muscles/group; #$p<0.05$ sex main effect.

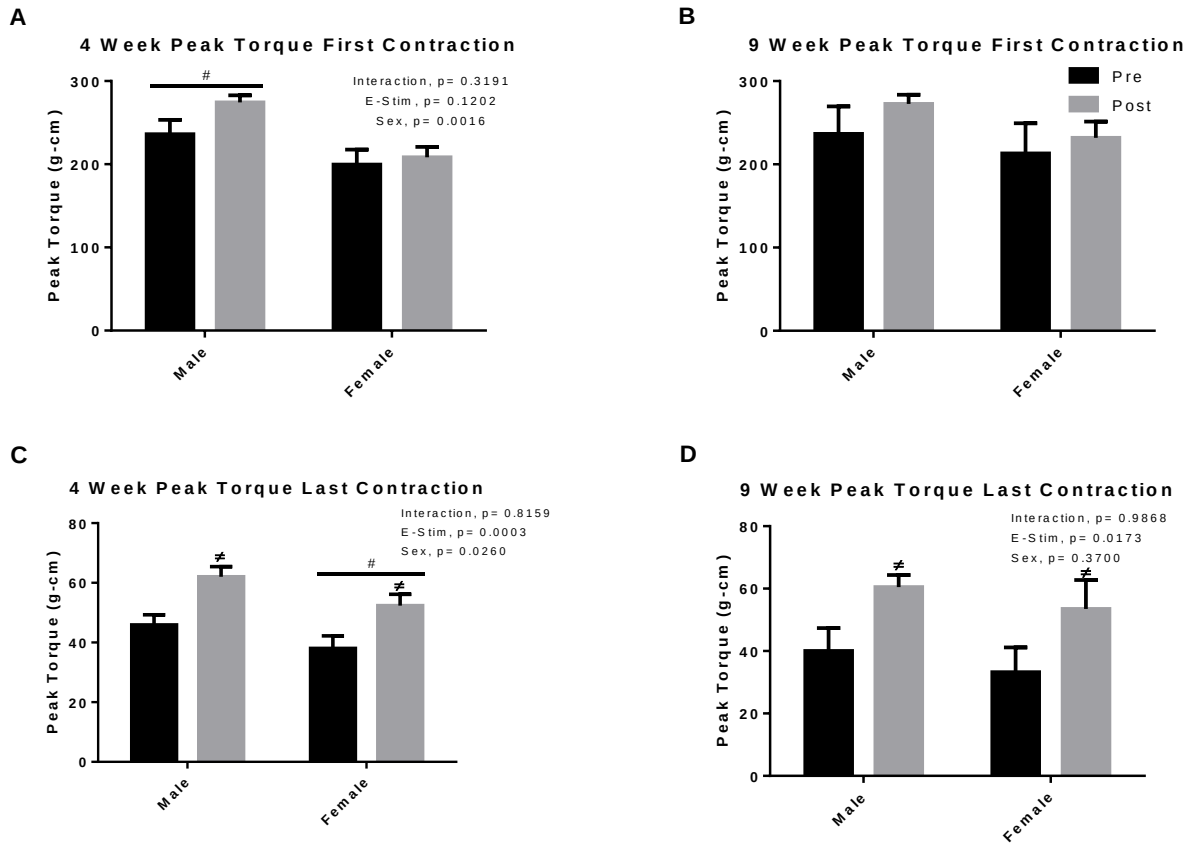

Figure 13 Peak torque for the first and last contractions in response to 4 and 9 weeks of electrical stimulation. Eight mice were subjected to 4 weeks of electrical stimulation twice weekly and six mice were subjected to 9 weeks of electrical stimulation twice weekly. Peak torque for the first eccentric contraction at 4 weeks **(A)** and 9 weeks **(B)**, peak torque for the last eccentric contraction at 4 weeks **(C)** and 9 weeks **(D)** before training and after training. Values are mean ± SEM. n = 7(A,C) and n=2-4(B,D) per group; ≠$p<0.05$ e-stim main effect, #$p<0.05$ sex main effect.

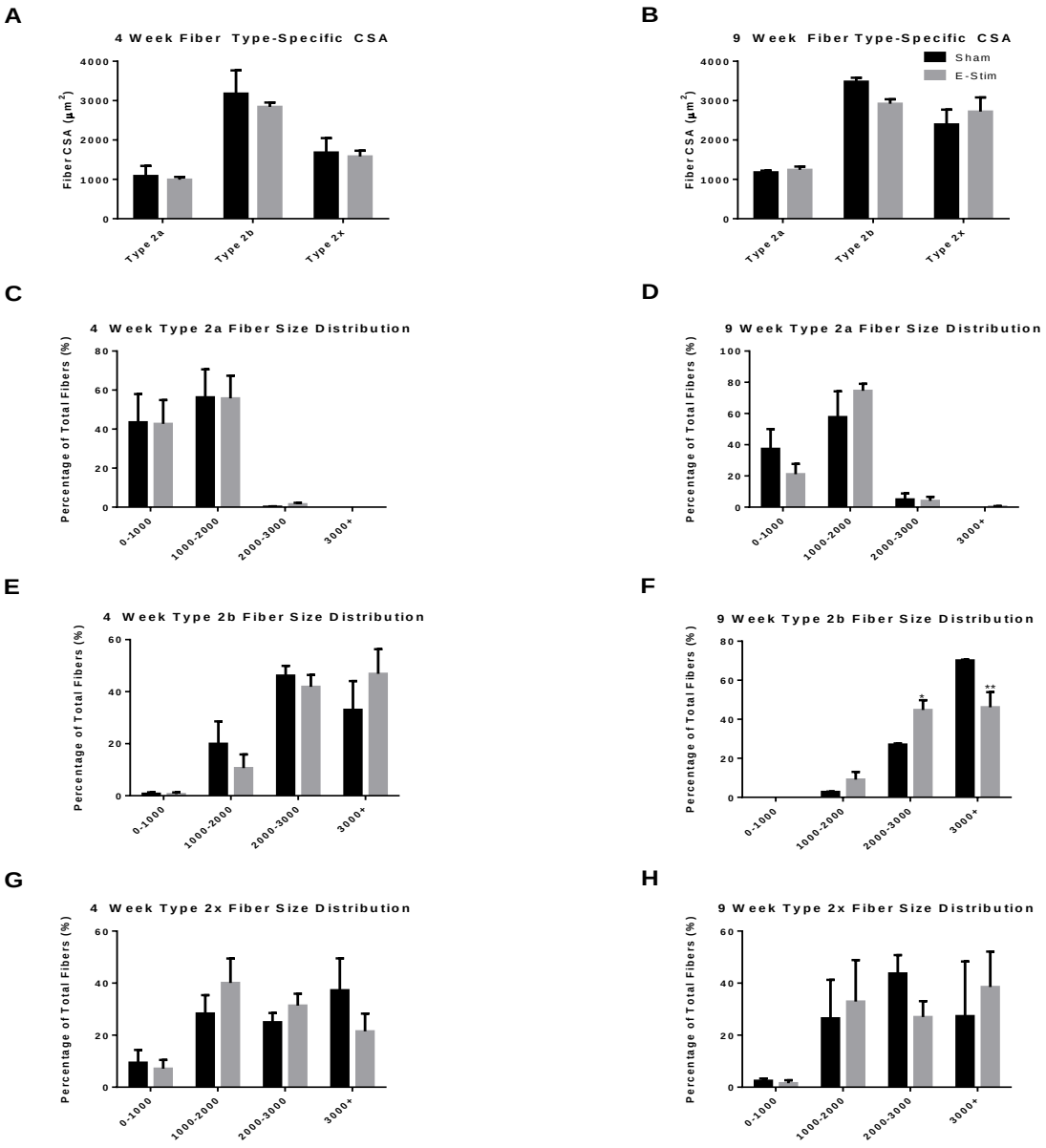

Figure 14 Muscle fiber type-specific size and distribution in response to 4 and 9 weeks of electrical stimulation. Eight 10 week-old mice were subjected to 4 weeks of electrical stimulation twice weekly and six 10 week-old mice were subjected to 9 weeks of electrical stimulation twice weekly. Gastrocnemius-soleus complexes were harvested and processed 24h after the last electrical stimulation bout. Fiber-type specific cross-sectional area at 4 weeks **(A)** and 9 weeks **(B)**, Type 2a fiber size distribution at 4 weeks **(C)** and 9 weeks **(D)**, Type 2b fiber size distribution at 4 weeks **(E)** and 9 weeks **(F)**, Type 2x fiber size distribution at 4 weeks **(G)** and 9 weeks **(H)**. Values are mean ± SEM. n = 4 (A,C,E,G), n = 2 (shams for B,D,F,H) muscles/group; *p<0.05 vs. 2000-3000 sham; **p<0.01 vs. 3000+ sham.

D) Flow Cytometry Analysis of the Skeletal Muscle Response to Repeated Electrical Stimulation.

Multiplex flow cytometry was used to examine pericyte quantity and cell surface phenotype in skeletal muscle following 4 weeks of repeated electrical stimulation. We assessed the percentage of $NG2^+$ (Figure 15A), $CD146^+$ (Figure 15B), $CD45^+CD31^+$ (Figure 15C) and $CD140A^+$ (Figure 15D) cells following stimulation compared to shams. Electrical stimulation training did not significantly alter the percentage of these cells at 4 weeks. No changes in $NG2^+$ or $NG2^+Lin^-$ cells were noted (Figures 15E-F). However, similar to the results from our acute study, expression of CD140A was increased in the $NG2^+CD45^-CD31^-$ pericyte fraction ($p<0.05$ vs. sham) (Figure 16A). The expression of CD140A did not change in the CD146+CD45-CD31- fraction with stimulation (Figure 16B). Lastly, expression of CD146 was not altered in $NG2^+CD45^-CD31^-$ pericytes after repeated electrical stimulation (Figure 16C).

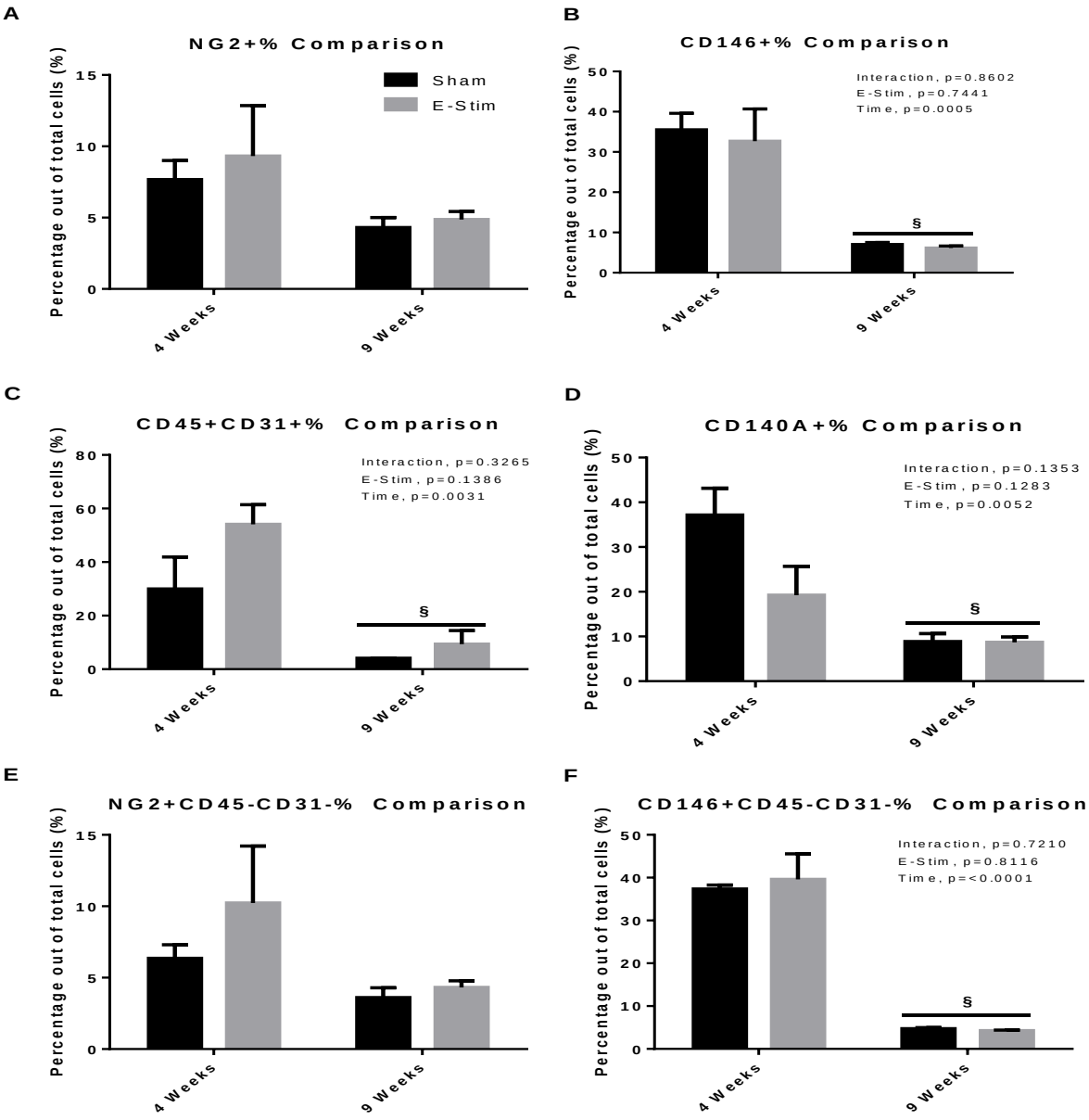

Figure 15 Flow cytometry analysis of the cell response to 4 and 9 weeks of electrical stimulation. Eight 10 week-old mice were subjected to 4 weeks of electrical stimulation twice weekly and six 10 week-old mice were subjected to 9 weeks of electrical stimulation twice weekly. Gastrocnemius-soleus complexes were harvested and processed 24h after the last electrical stimulation bout. $NG2^{+}$**(A)**, CD146+**(B)**, $CD45^{+}CD31^{+}$**(C)**, $CD140A^{+}$**(D)**, $NG2^{+}CD45^{-}CD31^{-}$**(E)**, and $CD146^{+}CD45^{-}CD31^{-}$**(F)** response to electrical stimulation training. Values are mean ± SEM. n = 2 (9 week shams) and n = 4 (4 week e-stim/shams and 9 week e-stim) muscles/group; §p<0.01 time main effect.

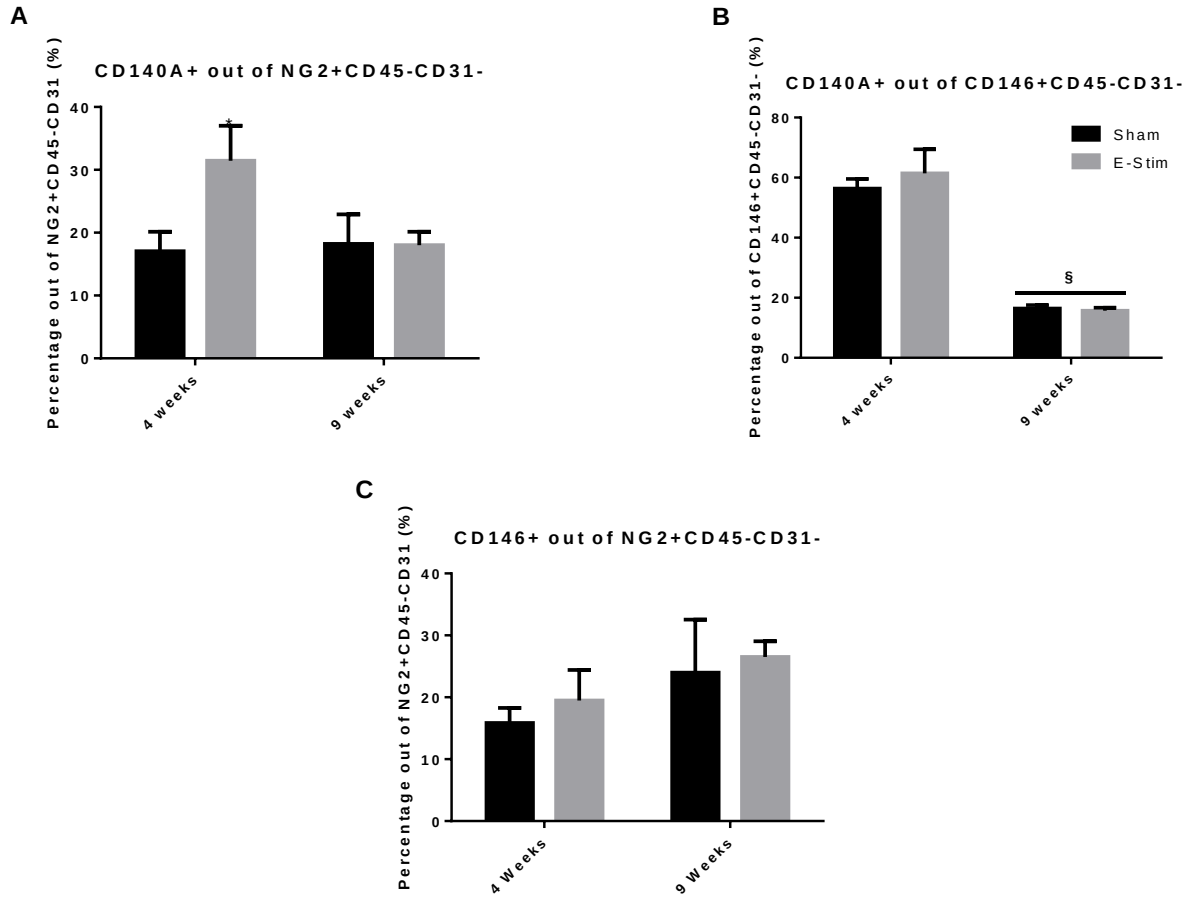

Figure 16 Flow cytometry analysis of the mononuclear cell content out of pericytes to 4 and 9 weeks of electrical stimulation. Eight 10 week-old mice were subjected to 4 weeks of electrical stimulation twice weekly and six 10 week-old mice were subjected to 9 weeks of electrical stimulation twice weekly. Gastrocnemius-soleus complexes were harvested and processed 24h after the last electrical stimulation bout. $CD140A^+$ percentage out of $NG2^+CD45^-CD31^-$ pericytes **(A)**, $CD140A^+$ percentage out of $CD146^+CD45^-CD31^-$ pericytes **(B)** and $CD146^+$ percentage out of $NG2^+CD45^-CD31^-$ pericytes **(C)** in response to electrical stimulation training. Values are mean ± SEM. n = 2 (9 week shams) and n = 4 (4 week e-stim/shams and 9 week e-stim) muscles/group; *$p<0.05$ vs. 4 week sham; §$p<0.01$ time main effect.

CHAPTER IV

DISCUSSION

Establishing a Resistance Exercise Model in Rodents

It is well established that chronic muscle contractions such as those induced by resistance exercise lead to beneficial adaptive responses in human skeletal muscle, such as myofiber hypertrophy and increased strength (Ogasawara, 2013; Damas, 2015). Resistance training using animal models is advantageous as it allows for tight experimental controls and whole-tissue analysis, which is harder to accomplish using human models. The application of resistance exercise in an animal model, specifically rodents, is highly problematic due to the inability of these models to properly engage in exercise in a manner similar to humans. Compared to other options (voluntary exercise, compensatory overload) electrical stimulation appears to provide the best option to mimic resistance exercise in humans, as it allows for implementation of specific exercise protocols and maximal activation of motor units independent of animal motivation (Lowe, 2002).

The results of eccentric-only electrical stimulation experiments demonstrate significant improvement in strength, likely due to neural adaptation (Ambrosio, 2012; Distefano, 2013). However, not all demonstrate an increase in muscle hypertrophy (Ambrosio, 2012; Distefano, 2013; Tsutaki, 2013). In the current study, our goal was to develop an electrical stimulation training protocol that would allow for both improvements in muscle strength and growth. Specifically, we sought to increase hypertrophy in the gastrocnemius-soleus muscle, the large muscle group that provides a large yield of stem cells via FACS. Our exact protocol included 8 alternating eccentric/concentric sets of 5 repetitions with a 10-second rest period between the sets (repeated twice weekly for the training studies). This protocol was designed with the hope

that inclusion of concentric contractions would prevent damage and improve capacity for growth. The results from our study suggested significant improvements in fatigue resistance, yet no increase in muscle mass (absolute or relative to body weight) or fiber-type specific changes in the mean myofiber CSA, including type 1 fibers that were minimally represented in our samples. Distribution by size also did not reveal any significant impact of training on myofiber hypertrophy. We suspect that lack of inclusion of a pulley system necessary to increase resistance to muscle force may be necessary to improve capacity for growth (Wong, 1988; Baar, 1999; McBride, 2003; McBride; 2006). In addition, it is possible that our protocol stimulated growth to a greater extent in other muscles, such as the TA, but other muscles were not evaluated. Therefore, optimization of the current electrical stimulation protocol will be necessary prior to conduction of experiments that will determine a role for the pericyte in resistance exercise-mediated muscle growth.

Pericyte to Mesenchymal Stem/Stromal Cell Transition

Caplan (2008) and Crisan (2008) both noted co-expression of CD90 and CD140A in pericytes and MSCs, an observation that led to a speculation of a link or phenotype switch amount the two subpopulations in skeletal muscle. A recent study conducted by Farup et al. demonstrated that $NG2^+$ and ALP^+ pericytes are significantly decreased in human skeletal muscle following 12 weeks of isolated concentric or eccentric contractions, as assessed in tissue sections using traditional immunofluorescence (Farup, 2015). The authors hypothesized that the decrease was due to a pericyte to MSC transition.

Thus, the current study was designed to assess not only pericyte quantity, but also the potential for pericytes to upregulate the MSC marker, CD140A, in the short time period following an acute bout of resistance exercise. The total percentage of $NG2^+$ and $NG2^+Lin^-$ cells

in skeletal muscle was similar, ~5%, suggesting that hematopoietic and endothelial cells are not highly represented in the $NG2^+$ fraction. Similarly, the total percentage of $CD146^+$ and $CD146^+Lin^-$ cells in skeletal muscle were approximately the same, ~50-60%. The fact that the $CD146^+$ fraction was substantially larger (10X larger) than the $NG2^+$ fraction, as well as the lack of CD146 expression in $NG2^+Lin^-$ cells (~10%) suggests that $CD146^+$ cells isolated from muscle may include cell types other than pericytes. Our representative flow cytometry plots demonstrate the potential for two populations of $CD146^+$ cells to be present in muscle, one that expresses CD146 to a higher extent than the other. It will be of interest to separate and characterize these fractions in the future to determine if differences exist between cell surface marker expression and phenotype. Although the total percentage of $NG2^+$ and $CD146^+$ pericytes (with and without Lin exclusion) was not significantly altered with acute electrical stimulation, the expression of CD140A was increased in both. Taken together, these data suggest that an acute bout of electrical stimulation does not stimulate the expansion of the pericyte population, but rather increases the potential for $NG2^+$ and $CD146^+$ pericytes to transition to an MSC phenotype. The lack of CD146 expression in the NG2 fraction also suggests that $NG2^+$ cells do not transition to $CD146^+$ cells post-stimulation.

The percentage of $NG2^+$ and $CD146^+$ pericytes in skeletal muscle did not change as a result of 4 or 9 weeks of repeated electrical stimulation, suggesting contraction does not appear to be a significant stimulus for pericyte expansion. However, CD140A remained elevated in the $NG2^+Lin^-$ fraction following 4 weeks of simulation. Only 30% of the fraction expressed CD140A at 4 weeks compared to 50% following an acute bout, and no change was observed by 9 weeks. These results suggest that adaptation may prevent the increase in CD140A expression with electrical stimulation. Unexpectedly, a significant drop in the $CD146^+$, $CD146^+Lin^-$, Lin^+

and $CD140A^+$ fractions was observed in the sham group at 9 weeks compared to 4 weeks, with no change observed in the stimulation group. The drop may represent an age-related phenomena, as mice were 5 weeks older (19 weeks of age vs. 14 weeks).

Previous work by Miller et al. (1995) demonstrated a significant decrease in pericyte quantity during a transition into adulthood, attributed to brain maturation and capillary quiescence compared to higher pericyte activity during development. However, since the $CD146^+$ fraction was predominantly affected compared to the $NG2^+$ fraction, it is possible that cells other than pericytes are transitioning to another cell type not examined in this study. Given the low number of samples evaluated at the 9 week time period (n=2-4 per group) in this preliminary study, it will be important to repeat these assessments in a follow up study.

Pericyte Gene Expression in Response to Acute Exercise

We attempted to acquire and analyze RNA from the $NG2^+CD45^-CD31^-$ pericyte population, but due to the rarity of these cells (<5% in this experiment), we were not able to extract enough RNA from our samples to successfully complete gene expression on this population. Thus, we chose to examine the $CD146^+CD45^-CD31^-$ pericyte response to acute simulation. We were highly interested in examining the potential for the cells to upregulate myogenic regulatory factors given the potential for these cells to engage in myogenesis and directly contribute to fiber repair/regeneration (Dellavalle, 2007). A significant increase in Myf5 relative mRNA expression and a trend for increase in MyoD relative mRNA expression was observed in female mice. We did include a primer set for myogenin in our assay. However, amplification was not successful in some of the samples and a conclusion regarding myogenin gene expression could not be made.

A variety of growth factors including HGF, LIF and IGF-1 stimulate satellite cell activation and/or differentiation (White, 1989; Miller, 2000; Munoz-Canoves, 2013). In the current study, growth factor gene expression was increased in $CD146^{+}Lin^{-}$ pericytes in a sex-dependent manner, such that both HGF and LIF were increased in females and IGF-1 was substantial increased in males post-stimulation. These data suggest the potential for these cells to indirectly contribute to skeletal muscle repair via activation of satellite cells.

Vascular-associated stem/stromal cells ($Sca\text{-}1^{+}CD45^{-}$) secrete paracrine factors necessary for extracellular matrix remodeling, including a wide variety of Mmp and Timp isoforms (Valero, 2012; De Lisio, 2014; Tokunaga, 2014). Timp1, Mmp2 and Mmp14 were significantly increased in response to acute stimulation, and these changes were predominant in the males. Thus, these cells likely contribute to the ECM remodeling event that has been observed following resistance training (Miller, 2005).

Although striking changes were observed in gene expression patterns related to myogenesis, growth factors, and ECM remodeling, relatively few changes were observed with regard to inflammatory cytokine or neurotrophic factor gene expression. In addition, with the exception of CD45 gene expression, which was increased in response to acute stimulation, no significant changes were noted with respect to cell surface marker gene expression. The change in CD45 gene expression is worth investigating in the future since protein expression was not able to be assessed with flow cytometry (due to the evaluation of both CD45 and CD31 on the same channel). Taken together, these data suggest that acute stimulation selectively regulates gene expression in the pericyte for the purpose of enhancing muscle repair and simultaneously remodeling the tissue environment to accommodate that process. The distinct changes in gene expression in females compared to males may reflect greater need for repair due to increased

strain-mediated damage in muscles of smaller size, or simply greater capacity for repair. We speculate that the increase in HGF and LIF may allow for optimal satellite cell expansion and repair in the females, whereas the increases in IGF-1 and ECM components may facilitate satellite cell differentiation and fusion with existing fibers in males.

Conclusion

This study provides the first evaluation of the pericyte response to a model of resistance exercise in mice. The results suggest that an acute bout of electrical stimulation does not increase pericyte quantity, but facilitates a transition to an MSC phenotype based on CD140A expression. In addition, results for high throughput qPCR suggest that while $NG2^{+}$ pericytes may not synthesize paracrine factor to a large extent, $CD146^{+}$ pericytes support muscle fiber repair and/or regeneration. Future studies will need to address CD146 heterogeneity given the relatively large fraction of cells expressing CD146 in muscle and the two distinct populations observed with flow cytometry. The extent to which these early changes in pericyte function provide the basis for beneficial adaptions with long-term resistance training is not clear, but our results demonstrate correlations with fatigue resistance following repeated bouts of electrical stimulation for 4 weeks. Future studies will focus on refining our model of resistance training so that a role for the pericyte in hypertrophy may be addressed.

REFERENCES

Adams, G.R., Caiozzo, V.J., Haddad, F., Baldwin, K.M. (2002). Cellular and molecular responses to increased skeletal muscle loading after irradiation. *Am J Physiol Cell Physiol, 283,* 1182-1195.

Adams, G.R., Cheng, D.C., Haddad, F., Baldwin, K.M. (2003). Skeletal muscle hypertrophy in response to isometric, lengthening, and shortening training bouts of equivalent duration. *J Appl Physiol, 96,* 1613-1618

Ambrosio, F., Fitzgerald, G.K., Ferrari, R., Distefano, G., Carvell, G. (2012). A murine model of muscle training by neuromuscular electrical stimulation. *Journal of Visualized Experiments, 63,* 1-6.

Amos, P.J., Shang, H., Bailey, A.M., Taylor, A., Katz, A.J., Pierce, S.M. (2008). IFATS Collection: the role of human adipose-derived stromal cells in inflammatory microvascular remodeling and evidence of a perivascular phenotype. *Stem Cells, 26,* 2682-2690.

Armulik, A., Genove, G., Betshotz, C. (2011). Pericytes: Developmental, physiological and pathologic perspectives, problems, and promises. *Developmental Cell, 21,* 193-215.

Baar, K., Esser, K. (1999). Phosphorylation of p70(s6k) correlates with increased skeletal muscle mass following resistance exercise. *Am J Physiol, 276,* 120-127.

Barash, I.A., Mathew, L., Ryan, A.F., Chen, J., Lieber, R.L. (2003). Rapid muscle-specific gene expression changes after a single bout of eccentric contractions in the mouse. *Am J Physiolog Cell Physiol, 286,* 355-364.

Birbrair, A., Zhang, T., Wang, Z., Messi, M.L., Enikolopov, G.N., Mintz, A., Delbono, O. (2013). Role of pericytes in skeletal muscle regeneration and fat accumulation. *Stem Cells and Development, 22*(16), 2298-2311.

Boppart, M.D., De Lisio, M., Zou, K., Huntsman, H.D. (2013). Defining a role for non-satellite stem cells in the regulation of muscle repair following exercise. *Frontiers in Physiology, 4*, 1-6.

Caplan, A.I. (2008). All MSCs are pericytes? *Cell Stem Cell, 11(*3), 229-230.

Cheek, D.B., Powell, G.K., Scott, R.E. (1965). Growth of muscle mass and skeletal collagen in the rat. *John Hopkins Hosp, 116,* 378-387.

Corona, B.T., Baloq, E.M., Doyle, J.A., Rupp, J.C., Luke, R.C., Inqalls, C.P. (2010). Junctophilin damage contributes to early strength deficits and EC coupling failure after eccentric contractions. *Am J Physiol Cell Physiol, 298,* 365-376.

Crisan, M., Yap, S., Casteilla, L., Chen, C., Corselli, M., Park, T.S., Andriolo, G., Sun, B., Zheng, B., Zhang, L. et al. (2008). A perivascular origin for mesenchymal stem cells in multiple human organs. *Cell Stem Cell, 3,* 301-313.

Crisan, M., Yap, S., Casteilla, L., Chen, C.W., Corselli, M., Park, T.S., Andriolo, G., Sun, B., Zheng B., Zhang, L., Norotte, C., Teng, P.N., Traas, J., Schugar, R., Deasy, B.M., Badylak, S., Buhring, H.J., Giacobino, J.P., Lazzari, L., Huard, J., Peault, B. (2008). A perivascular origin for mesenchymal stem cells in multiple organs. *Cell Stem Cell, 11*(3), 301-313.

Damas, F., Phillips, S., Vechin, F.C., Ugrinowitsch, C. (2015). A review of resistance training-induced changes in skeletal muscle protein synthesis and their contribution to hypertrophy. *Sports Med, 45*, 801-807.

De Lisio, M., Jensen, T., Sukiennik, R.A., Huntsman, H.D., Boppart, M. (2014). Substrate and strain alter the muscle-derived mesenchymal stem cell secretome to promote myogenesis. *Stem Cell Res Ther, 5,* 74.

Dellavalle, A., Sampaolesi, M., Tonlorenzi, R., Tagliafico, E., Sacchetti, B., Perani, L., Innocenzi, A., Galvez, B.G., Messina, G., Morosetti, R., Li, S., Belicchi, M., Peretti, G., Chamberlain, J.S., Wright, W.E., Torrente, Y., Ferrari, S., Bianco, P., Cossu G. (2007). Pericytes of human skeletal muscle are myogenic precursors distinct from satellite cells. *Nat Cell Biol, 9,* 255-267.

Distefano, G., Ferrari, R.J., Weiss, C., Deasy, B.M., Boninger, M.L., Fitzegerald, G.K., Huard, J., Ambrosio, F. (2013). Neuromuscular electrical stimulated as a method to maximize the beneficial effects of muscle stem cells transplanted into dystrophic skeletal muscle. *PLOS One, 8,* 1-11.

Farup, J., De Lisio, M., Rahbek, S., Bjerre, J., Vendelbo, M., Boppart, M.D., Vissing, K. (2015). Pericyte response to contraction mode-specific resistance exercise training in human skeletal muscle. *J Appl Physiol, 119,* 1053-1065.

Fry, C.S., Lee, J.D., Jackson, J.R., Kirby, T.J., Stasko, S.A., Liu, H., Dupont-Versteegden, E.E., McCarthy, J.J., Peterson, C.A. (2014). Regulation of the muscle fiber microenvironment by activated satellite cells during hypertrophy. *FASEB J, 28,* 1654-1665.

Heredia, J.E., Mukundan, L., Chen, F.M., Mueller, A.A., Deo, R.C., Locksley, R.M., Rando, T.A., Chawla, A. (2013). Type 2 innate signals stimulate fibro/adipogenic progenitors to facilitate muscle regeneration. *Cell, 153,* 376-388.

Hirschi, K.K., D'Amore, P.A. Pericytes in the microvasculature. (1996). *Cardiovasc. Res., 32,* 687-698.

Hunstman, H.D., Zachwieja, N., Zou, K., Ripchik, P., Valero, M.C., De Lisio, M., Boppart, M.D. (2013). Mesenchymal stem cells contribute to vascular growth in skeletal muscle in response to eccentric exercise. *Am J Physiol Heart Circ Physiol, 304,* H72-H81.

Joe, A.W., Yi, L., Natarajan, A., Le Grand, F., So, L., Wang, J., Rudnicki, M.A., Rossi, F.M. (2010). Muscle injury activates resident fibro/adipogenic progenitors that facilitate myogenesis. *Nat Cell Biol, 12,* 153-163.

Kostallari, E., Baba-Amer, Y., Alonso-Martin, S., Ngoh, P., Relaix, F., Lafuste, P., Gherardi, R.K. (2015). Pericytes in the myovascular niche promote post-natal myofiber growth and satellite cell quiescence. *Stem Cells and Regeneration*, *142,* 1242-1253.

Lowe, D.A, Alway, S.E. (2002). Animal models for inducing muscle hypertrophy: are they relevant for clinical applications in humans? *Journal of Orthopedic & Sports Physical Therapy, 32,* 36-43.

McBride, T.A. (2003). Stretch-activated ion channels and c-fos expression remain active after repeated eccentric bouts. *J Appl Physiol, 94,* 2296-2302

McBride, T.A. (2006). AT1 receptors are necessary for eccentric training-induced hypertrophy and strength gains in rat skeletal muscle. *Ex Physiol, 91,* 413-421.

McCarthy, J.J., Mula, J., Miyazaki, M., Erfani, R., Garrison, K., Farooqui, A.B., Srikuea, R., Lawson, B.A., Grimes, B., Keller, C., Van Zant, G., Campbell, K.S., Esser, K.A., Dupont-Versteegden, E.E., Peterson C.A. (2011). Effective fiber hypertrophy in satellite cell-depleted skeletal muscle. *Development, 138,* 3657-3666.

Miller, B., Sheppard, A., Bicknese, A., Perlman, A. (1995). Chondroitin sulfate proteoglycans in the developing cerebral cortex: The distribution of neurocan distinguishes forming afferent and efferent axonal pathways. *J Comp Neurol, 355,* 615-628.

Miller, K.J., Thaloor, D., Matteson, S., Pavlath, G.K. (2000). Hepatocyte growth factor affects satellite cell activation and differentiation in regenerating skeletal muscle. *Am J Physiol Cell Physiol, 278,* 174-181.

Miller, B.F., Olesen, J.L., Hansen, M., Dossing, S., Crameri, R.M., Welling, R.J., Langberg, H., Flyvbjerg, A., Kjaer, M., Babraj, J.A., Smith, K., Rennie, M.J. (2005). Coordinated collage and muscle protein synthesis in human patella tendon and quadriceps muscle after exercise. *J Physiol, 567,* 1021-1033.

Mills, S.J., Cowin, A.J., Kaur, P. (2013). Pericytes, mesenchymal stem cells and the wound healing process. *Cells, 2,* 621-634.

Morgan, D.L., Proske. U. (2001). Muscle damage from eccentric exercise: mechanism, mechanical signs, adaptation and clinical applications. *Journal of Physiology, 537,* 333-345.

Munoz-Canoves, P., Scheele, C., Pedersen, B.K., Serrano, A.L. (2013). Interleukin-6 myokine signaling in skeletal muscle: a double-edged sword? *FEBS Journal, 280,* 4131-4148.

Ogasawara, R., Sato, K., Matsutani, K., Nakazato, K., Fujita, S. (2014). The order of concurrent endurance and resistance exercise modifies mTOR signaling and protein synthesis in rat skeletal muscle. *Am J Physiol Endocrinol Metab, 306,* 1155-1162.

Ozerdem, U., Grako, K.A., Dahlin-Huppe, K., Monosov, E., Stallcup, W.B. (2001). NG2 Proteoglycan is expressed exclusively by mural cells during vascular morphogenesis. *Dev. Dyn., 222,* 218-227.

Relaix, F., Zammit, P.S. (2012). Satellite cells are essential for skeletal muscle regeneration: The cell on the edge returns centre stage. *Development, 139,* 2845-2856.

Snijders, T., Verdijk, L.B., McKay, B.R., Smeets, J.S., van Kranenburg, J., Groden, B.B., Parise, G., Greenhaff, P., van Loon, L.J. (2014). Acute dietary protein intake restriction is associated with changes in myostatin expression after a single bout of resistance exercise in health young men. *J Nutr, 144(*2), 137-145.

Tokunaga, M., Inoue, M., Jiang, Y., Barnes, R.H., Buchner, D.A., Chun, T.H. (2014). Fat depot-specific gene signature and ECM remodeling of Sca1(high) adipose-derived stem cells. *Matrix Biol, 36,* 28-38.

Tsutaki, A., Ogasawara, R., Kobayashi, K., Lee, K., Kouzaki, K., Nakazato, K. (2013). Effect of intermittent low-frequency electrical stimulation on rat gastrocnemius muscle. *BioMed Research International,* 1-9.

Valero, M.C., Huntsman, H.D., Liu, J., Zou, K., Boppart, M.D. (2012). Eccentric exercise facilitates mesenchymal stem cell appearance in skeletal muscle. *PLoS ONE, 7:*e29760.

White, T.P., Esser, K.A. (1989). Satellite cell and growth factor involvement in skeletal muscle growth. *Med Sci Sports Exerc, 21,* 158-163.

Wong, T.S., Booth, F.W. (1988). Skeletal muscle enlargement with weight-lifting exercise by rats. *J Appl Physiol, 65,* 950-954.

Yang, Y., Creer, A., Jemiolo, B., Trappe, S. (2005). Time course of myogenic and metabolic gene expression in response to acute exercise in human skeletal muscle. *Journal of Applied Physiology, 98,* 1745-1752.

Zammit, P.S., Relaix, F., Nagata, Y., Ruiz, A.P., Collins, C.A., Partridge, T.A., Beauchamp, J.R. (2006). Pax7 and myogenic progression in skeletal muscle satellite cells. *J Cell Sci, 119,* 1824-1832.

Zou, K., Hunstman, H.D., Valero, C.M., Adams, J., Skelton, J., De Lisio, M., Jensen, T., Boppart, M.D. (2015). Mesenchymal stem cells augment the adaptive response to eccentric exercise. *Med Sci Sports Exerc, 47,* 315-325.

APPENDIX: Experimental Protocols

A) RNA Quantification

a. Clean Biotech before use
    i. Add 2 uL of RNase free water to each well, then **blot dry** and wipe down opposite glass cover
b. Nucleic acid quantification set up
    i. Add 2 uL of RNase free water to first to wells in A
    ii. Close cover slowly (magnetic seal will pull down cover, do so gently as not to disturb samples)
    iii. Place in plate reader and open Gen5 software, and select Nucleic acid quantification program
    iv. Run program and validate with the blanks until image turns up green (acceptable CV percentage)
c. Blot dry again
d. Add 2 uL of sample to each well (see below) and close cover
e. Run plate in plate reader and export data to Excel
f. Reclaim the 2 uL of sample from well (and any on the glass cover)
g. Blot dry with RNase free water and wipe down glass cover.
h. Repeat process with remainder of sample
    i. For any samples with differences > 5ng/uL repeat analysis of that sample once done with all samples
i. Save Excel data and email to yourself for later usage

B) RNA Extraction from Lysed Cells:

1. Add equal volume of **70% EtOH** to volume of sample, and mix by inversion/pipetting
2. Add **700µL of 70% EtOH**-sample mix to spin column
    a. Centrifuge @ **10,000 RPM** (≥8,000g) for **15 sec @ room temperature (RT)**
    b. Discard flow through into organic waste bottle
        i. Flow through can also be saved for protein extraction by Acetone precipitation
3. Add **350µL of RW1 buffer** to spin column
    a. Centrifuge @ **10,000 RPM for 15 sec @ RT**
    b. Discard flow through
4. Prepare DNase Mix
    a. Add **10µL of DNase I stock to 70µL Buffer RDD** – Mix by gentle inversion
5. Add **80µL DNase I Incubation Mix** into each spin column and **incubate @RT for 15'** (<u>pipette directly on membrane</u>)
6. Add **350µL of RW1 buffer** to spin column
    a. Centrifuge @ **10,000 RPM for 15sec @ RT**
    b. Discard flow through ***<u>and</u>*** collection tube
7. Add **500mL of RPE Buffer** to spin column
    a. Centrifuge @ **10,000 RPM for 15 sec @ RT**
    b. Discard flow through
8. Add **500µL of 80% EtOH** to Spin Column

a. Centrifuge **@ 10,000 RPM for 2' @ RT**
b. Discard flow through *and* collection tube

9. Put the spin column in new 2 mL collection tube
10. Spin at **full speed for 5'** with lids of spin columns open (to dry residual EtOH)
    a. Discard flow through *and* collection tube
11. Put the spin column in new **capped 2 mL collection tube**
    a. Pipette **14µL of RNase free water** *directly onto the membrane*
    b. Centrifuge @ **10,000 RPM for 1' @RT**
    c. DO NOT DISCARD – This is the RNA sample!
    d. Repeat a-c with the same 14µL RNase free water (optional)
    e. Discard spin column and **store collection tube in -80°C freezer**

C) RT-PCR

1. Create plate outline for sample and gene organization.

	1 well (uL)	**# of wells (uL)**
Taqman Primer	0.5	**0.5*#**
Taqman Master Mix	5.0	**5.0*#**

2. Thaw samples in fridge
3. Calculate PCR Master Mix volume per gene (solutions in fridge)
    a. # of wells per gene = # of samples x replicates +2-4 extra

4. PCR Master Mix quantities per gene:
    a. Volume of Primer: **0.5 uL * #of wells**
    b. Vol. Master Mix: **5.0 uL * #of wells**
    c. Combine Primer and Master Mix into appropriate sized eppendorf tube
    d. Repeat for each gene
5. Add **5.5 uL of PCR Master Mix** to each well for that gene
6. Add **4.5 uL of cDNA sample** to each well
7. If possible, include negative control (Master Mix + RNase free water) for each gene [duplicate] to assess contamination
    a. Once completed, seal with cover and wrap in aluminum (protects fluorophores from light) and store in fridge until taken to Functional Genomic Center for analysis

D) PCR Pre-Amplification

1. Begin thawing cDNA samples and needed primers in fridge
2. **Calculate cDNA and H2O volume to add**:
   - Vol. of cDNA to equal 1-250ng per sample
   - 12.5uL – cDNA vol. = RNase-free water volume
3. Make PreAmp Master Mix in 1.5mL eppendorf tube:

Master Mix:

   - Taqman PreAmp Mix = 25uL * # rxns
   - Pooled Primer Volume = 12.5uL * # rxns
     - Individual Primer Volume = PPV/100
     - TE Buffer = PPV – (#primers * IPV)
   - RNase-free water = Vol. uL * # rxns
   - Number of primers = # primers
4. Add **# uL cDNA** sample to 200uL tubes
5. Add appropriate vol of Master Mix to each sample for a total **50uL/sample tube**
6. Spin down tubes to remove air bubbles
7. Place in Thermocycler and run appropriate program:
   a. User name: Yair
   b. Program name: Exp001 (see below to confirm set-up)
   c. Run program
8. Add 950uL of DEPC+RNase-free water to 50 uL of PreAmp solution
9. Store in -20^{o}C freezer

E) PCR Analysis

1. Use SDS 2.4 and obtain CT values for each sample per gene
2. Export data as text file and copy/paste to an Excel spreadsheet
3. Calculate fold change for each sample and gene using ΔΔCT Method

δδCT Method:

A. In Excel, format a replica of the PCR plate
B. Copy/paste each CT value to appropriate cell to match plate format
C. Average each CT value per gene per sample
D. Copy values to new sheet and format according to gene and sample label
E. In another sheet, copy/paste the CT values for housekeeping gene (i.e. GAPDH) per sample
F. Choose a gene to analyze and copy/paste CT values
G. Choose a reference sample with which to compare other samples
H. Calculate ΔCT value for reference sample, and average value
   a. This value is your **average reference ΔCT** to compare with remaining samples
I. Calculate **ΔΔCT value** by subtracting δCT from **the average reference ΔCT**
   a. δCT of Sample A – Average δCT of Reference Sample
J. Determine **2^-(ΔΔCT) value** per sample

K. Average **2^-(ΔΔCT) value**
L. Calculate standard deviation (**SD**)
M. Calculate standard error mean (**SEM**)
    a. SD/sqrt(n)
N. Copy/paste **2^-(ΔΔCT) value average** and **SEM** to new sheet
O. Create bar graphs with error bars

F) Reverse Transcription of cDNA following Quantification

1. Average concentration values of each sample and record value (2 decimal places)
2. Average 260/280 ratio value per sample to determine purity
3. Total RNA Assessment
    a. Choose a volume 2-4 uL away from RNA volume attained from RNA extraction (see protocol, generally 14 uL total)
        i. i.e. 10 uL and 12 uL for total RNA concentrations
    b. Multiple RNA concentration by the proposed volume to determine total RNA (ng)
        i. Example:

            Sample concentration = 100 ng/uL

            Proposed volume = 12 uL

            Total RNA for sample = 100 ng/uL X 12 uL = **1200 ng/sample**

4. RT of cDNA calculations
    a. Determine amount of RNA (ng) to use per sample so the total volume of sample is 10 uL (uL sample + uL RNase free water)
        i. Between 200-500 ng RNA if possible
    b. Make up 2x RT-Master mix (per 20 uL rxn)
5. Add 10 uL of Master mix to 10 uL of RNA sample+water into 0.2 microtube, pipetting up and down 2x to mix
6. Centrifuge tubes down to eliminate air bubbles
7. Place microtubes into thermal cycler, and program cycle as follows (with volume = 20 uL):
8. Run RT program
    a. Store at 4 °C short term or -20

G) MHC 2x and 1 Immunohistochemistry

1. 10 μm sections from cryostat were fixed immediately with –30 °C acetone for total 10 min, and stored inside –80 °C freezer before staining.
2. Wash with 1 X PBS 3 times for 5 mins.
3. Switch to incubation with 0.5% BSA and 0.5 % Triton-X plus **Fab anti-mouse IgG(1:10) (AffiniPure Fab Fragment Goat Anti-Mouse IgG (H+L) Jackson #115- 007-003)** for 1hr at room temperature
4. Wash with 3X5 min changes of PBS.
5. Primary AB Incubation conditions.
   -Mouse IgG2b anti-type I MHC antibody (BA-D5-supernatent from Developmental Studies Hybridoma Bank at the University of Iowa (1:20))

   -Mouse IgM anti-type 2x MHC antibody (6H1-supernatent from Developmental Studies Hybridoma Bank at the University of Iowa (1:20) (28μg/μL))

   - Rabbit anti-mouse dystrophin (Abcam ab15277, 1:100) in PBS containing 0.5 % BSA and 0.5 % Triton-X for 1 hr room temperature

6. Wash with 3X5 min changes of PBS.
7. Secondary AB Incubate conditions.:
   - Alexa 350 conjugated anti-mouse IgG2b 1:100 (Invitrogen Cat# A21140, UV-blue)

   -Alexa 488 anti-mouse IgM μ chain specific 1:100 (JacksonImmuno 115-545-075),

   - Alexa Fluor 633 goat anti rabbit (Invitrogen, 1:200) in PBS containing 0.5 % BSA and 0.5 % Triton-X for 1 hr room temperature.

8. Rinse in PBS (3X5 min).

H) MHC 2a and 2b Immunohistochemistry

a) 10 μm sections from cryostat were fixed immediately with –30 °C acetone for total 10 min, and stored inside –80 °C freezer before staining.

b) Let sections warm at room temperature for 5 min.

c) Wash with 1 X PBS 3 times for 5 mins.

d) Switch to incubation with 0.5% BSA and 0.5 % Triton-X plus **Fab anti-mouse IgG(1:10) (AffiniPure Fab Fragment Goat Anti-Mouse IgG (H+L) Jackson #115- 007-003)** –for 1hr at room temperature

e) Wash with 3X5 min changes of PBS.

f) Primary AB Incubation conditions.

g) -Mouse IgM anti-type 2b MHC antibody (BF-F3-concentrate from Developmental Studies Hybridoma Bank at the University of Iowa (1:50, fridge))

h) -Mouse IgG1 anti-type 2a MHC antibody (Sc-71-supernatent from Developmental Studies Hybridoma Bank at the University of Iowa (1:50, fridge)

i) Rabbit anti-mouse dystrophin (Abcam ab15277, 1:100) in PBS containing 0.5 % BSA and 0.5 % Triton-X for 1 hr room temperature

j) Wash with 3X5 min changes of PBS.

k) Secondary AB Incubate conditions:

l) -AMCA conjugated anti-mouse IgM u chain specific (Jackson Immunoresearch Cat#115-155-075, 1:100, UV-blue, Freezer box#3),

m) -Alexa 488 conjugated anti-mouse IgG subclass 1 (Jackson Immunoresearch Cat#115-545-205, 1:100, green).

n) Alexa Fluor 633 goat anti rabbit (Invitrogen, 1:200) in PBS containing 0.5 % BSA and 0.5 % Triton-X for 1 hr room temperature.

o) Rinse in PBS (3X5 min).

I) Cell Isolation for Flow Cytometry and Gene Expression

Day before: Prepare solutions, antibody mixes and autoclave tools.

Muscle Cell isolation for Flow Cytometry:

1. Pipet 1-2 mL of PBS + P/S solution in small petri dishes to collect the harvested muscles.

2. Sacrifice mice, record body weight and harvest the gastrocnemius. Weigh the muscle tissue and place muscle in the petri dish containing PBS + P/S.

3. Begin warming the enzyme solution in the water bath.

4. Transfer muscles to a 60mm petri dish containing 500µL per muscle of PBS + P/S.

Mince and Digest Muscle Tissue

5. Using autoclaved tools, mince the muscles extensively to increase surface area for collagenase digestion.

6. Add Collagenase and DNase to the warm enzyme solution. Add ~6mL of the enzyme solution per muscle to the petri dish and use a 25mL pipette to transfer the minced muscle into a 50mL tube.

7. Begin warming the inhibition medium.

8. Incubate the minced muscle for 45 mins in the water bath. Every 15 mins, titrate the solution using a 10mL pipette, working down to 5mL and 1000 µL pipette as the tissue becomes more digested.

9. Begin soaking 70µm and 40µm filters in a petri dish in PBS + P/S.

10. Filter the digested muscle solution through the 70µm followed by a 40µm filter. Add an equal volume of inhibition medium to stop the digestion.

Count Cells

11. Collect 10µL of solution from each sample into an Eppendorf tube for cell counting.

12. Centrifuge the samples for 5 mins at 450 RCF.

13. Cell counting: Add 10µL of trypan blue to the cell suspension from step 11. Mix well. Add 10uL of the resulting solution to a hemacytometer. Blue cells are dead cells.

Count the center square and the 4 corner squares. Average the 5 counts. *We typically get 1.5 x 10^6 cells from Sed and 3 x 10^6 from e-stim samples.*

Count Average * 10,000 * 2 = _____ cells/ml
_____ Cells /ml * total volume = _____ cells
Resuspension volume = _____ cells / 1.5 x 10^6 = _____ mL

14. Remove supernatant and resuspend the cell pellet in 2% FBS in PBS using the volumes obtained from step 13. Break any cell clumps by pipetting up and down using a 200 µL pipette.

Block the Fc receptor

15. Transfer 1 mL of solution to an Eppendorf tube. Add 5 µL of CD16/CD32 blocking antibody per 1 mL of cell suspension and incubate in the fridge on the rotator for 10 mins.

16. *Wash 1:* Add 500µL of 2% FBS + PBS to the blocking solution and centrifuge for 5 mins at 450 RCF.

17. *Wash 2:* Remove supernatant and resuspend the pellet in 1mL of 2% FBS + PBS. Break any cell clumps by pipetting up and down using a 200 µL pipette.

Stain the cells using Antibody Mix

18. Add 100µL of the cell suspension to the FMO antibody mixes and 200 µL to the Single stain and the sample tubes.

19. Incubate on ice in the rotator for 1 hour.

20. *Wash 1:* Add 1 mL of 2% FBS + PBS to the tubes and centrifuge for 5 mins at 450 RCF.

21. *Wash 2:* Resuspend the pellet in 1 mL of 2% FBS + PBS and centrifuge again for 5 mins at 450 RCF. Break any cell clumps by pipetting up and down using a 200 µL pipette.

Transfer to sort tubes:

22. Resuspend the pellet in 300 µL of 2% FBS + PBS and transfer to the sort tubes and place on ice.

23. Run the samples on the flow cytometer.